ENHANCEMENT OF EXISTING ENGINEERING SOFTWARE

VOLUME NO. 5

Transverse Load Distribution in Slab-girder Bridges

T. R. Finch
J. A. Puckett

Department of Civil Engineering
University of Wyoming
Laramie, Wyoming 82071

July, 1992

Technical Report Documentation Page

1. Report No. MPC92-9 Volume 5	2. Government Accession No.	3. Recipient's Catalog No.
4. Title and Subtitle Enhancement of Existing Engineering Software Volume No. 5 Transverse Load Distribution in Slab-girder Bridges		5. Report Date July 1992 6. Performing Organization Code
7. Author(s) T.R. Finch and J.A. Puckett		8. Performing Organization Report No.
9. Performing Organization Name and Address University of Wyoming Laramie, WY		10. Work Unit No. (TRAIS) 1. Contract or Grant No.
12. Sponsoring Agency Name and Address Mountain-Plains Consortium North Dakota State University Fargo, ND		13. Type of Report and Period Covered Project Technical Report 14. Sponsoring Agency Code

15. Supplementary Notes

Supported by a grant from the U.S. Department of Transportation, University Transportation Centers Program

16. Abstract

The finite strip method was used to develop an automated procedure for determining the distribution of load on highway bridges subjected to both standard truck loads and overload permit vehicle loads. The distribution factors obtained by this procedure are used in the design and load rating of highway bridges. Several verification problems were used to compare the automated procedure to closed-form solutions available from the theory of plates and shells. In addition, distribution factors from the numerical procedure were compared to various simplified methods for determining load distribution in highway bridges.

17. Key Words finite strip, bridge overload, slab-girder, load distribution	18. Distribution Statement		
19. Security Classif. (of this report)	20. Security Classif. (of this page)	21. No. of Pages 128	22. Price

ACKNOWLEDGEMENT

This report has been prepared with funds provided by the United States Department of Transportation to the Mountain–Plains Consortium (MPC). The MPC member universities include North Dakota State University, Colorado State University, University of Wyoming and Utah State University.

PREFACE

The primary objective of MPC 007 is to provide a methodology to enhance applications based on existing code. These methodologies were employed to enhance a finite strip program for the analysis of slab–girder bridges to determine how the load distributes to each girder and report the distribution factors necessary for design or rating. The Intergraph version of this application illustrates the methodology while providing the bridge engineer with a useful analysis tool. This report outlines the theory and application of the finite strip method and illustrates the use of the application with several examples. The report is intended for bridge engineers interested in the load distribution application and does not focus specifically on the methodology used to develop the application's user interface.

This application is one of several written or enhanced to illustrate the methodologies developed as part of MPC 007. Other applications include: BRASS–Girder (bridge design and rating), BRASS–Screed (girder profiles, screed elevations, slab thickening diagrams), BRASS–Culvert (Reinforced Concrete Culvert Design), and BRASS–Bearing (Elastomeric Bearing Design).

ABSTRACT

The finite strip method was used to develop an automated procedure for determining the distribution of load on highway bridges subjected to both standard truck loads and overload permit vehicle loads. The distribution factors obtained by this procedure are used in the design and load rating of highway bridges. Several verification problems were used to compare the automated procedure to closed–form solutions available from the theory of plates and shells. In addition, distribution factors from the numerical procedure were compared to various simplified methods for determining load distribution in highway bridges.

TABLE OF CONTENTS

CHAPTER	PAGE
1. INTRODUCTION	1
1.1. GENERAL	1
1.2. PRINCIPLES OF LOAD DISTRIBUTION	2
1.3. TRUCK LOADS ON HIGHWAY BRIDGES	5
1.3.1. STANDARD TRUCK LOADS	5
1.3.2. PERMIT VEHICLE LOADS	6
1.4. REVIEW OF CURRENT LITERATURE	9
1.4.1. AASHTO METHOD	9
1.4.2. NCHRP PROJECT 12–26	11
1.4.3. ONTARIO HIGHWAY BRIDGE DESIGN CODE	16
1.4.4. OTHER METHODS	20
1.5. OBJECTIVES AND SCOPE	23
2. GENERAL THEORY AND FORMULATION OF THE FINITE STRIP METHOD	25
2.1. INTRODUCTION	25
2.2. CHOICE OF DISPLACEMENT FUNCTIONS	28
2.2.1. SHAPE FUNCTION PART OF DISPLACEMENT FUNCTION	29
2.2.2. SERIES PART OF DISPLACEMENT FUNCTION	33
2.3. MATRIX FORMULATION	35
2.3.1 DISPLACEMENT FUNCTIONS	36
2.3.2. STRAINS	37
2.3.3. STRESSES	38
2.3.4. MINIMIZATION OF TOTAL POTENTIAL ENERGY	39
2.4. STIFFNESS CONTRIBUTION OF AN ELASTIC BEAM	43
2.5. APPLICATION OF THE FINITE STRIP METHOD	47

CHAPTER PAGE

3. VERIFICATION PROBLEMS 48
3.1. RECTANGULAR PLATE SIMPLY SUPPORTED ON TWO EDGES 48
3.2. SQUARE PLATE SIMPLY SUPPORTED ON TWO EDGES WITH THE OTHER TWO EDGES SUPPORTED BY ELASTIC BEAMS 59
3.3. SIMPLY SUPPORTED SINGLE STRIP WITH A CENTRALLY LOCATED BEAM 64
3.4. CONVERGENCE OF DISTRIBUTION FACTORS 68

4. COMPARISON OF DISTRIBUTION FACTORS FOR AN ILLUSTRATIVE EXAMPLE 69
4.1. EFFECTS OF SLAB THICKNESS AND SPAN LENGTH 69
4.2. EFFECTS OF SINGLE AND MULTIPLE LANE LOADING 75
4.3. DISTRIBUTION FACTORS FOR A PERMIT VEHICLE 81

5. SUMMARY AND CONCLUSIONS 84
5.1. SUMMARY 84
5.2. CONCLUSIONS 85
5.3. RECOMMENDATIONS FOR FUTURE RESEARCH 87

APPENDIX A 90

APPENDIX B 92

ENDNOTES 124

SELECTED BIBLIOGRAPHY 127

LIST OF FIGURES

FIGURE		PAGE
Figure 1.1.	Load Distribution in Girders Connected by One Transverse Beam (from Bakht and Moses (5)).	3
Figure 1.2.	Load Distribution in Girders Connected by Three Transverse Beams (from Bakht and Moses (5)).	4
Figure 1.3.	Shape of Bending Moment Diagrams (from Bakht and Moses (5)).	5
Figure 1.4.	Standard AASHTO HS Truck (Figure 3.7.7A from AASHTO *Standard Specifications for Highway Bridges*, 13th Edition (1989)).	6
Figure 1.5.	Permit Vehicle with an indivisible piece of cargo.	7
Figure 1.6.	Overweight Permit Vehicle.	8
Figure 1.7.	Design charts for determining values of D and C_f for a two lane bridge (reproduced from *Ontario Highway Bridge Design Code (1983)*).	19
Figure 2.1.	Discretization of a continuum into a finite number of strips.	27
Figure 2.2.	Typical finite strip with simple support conditions.	28
Figure 2.3.	Displacement field for a simply supported finite strip.	30
Figure 2.4.	Shape functions of a third-order polynomial fitted to ordinates and slopes at $x=0$ and at $x=b$.	33
Figure 2.5.	Typical finite strip supported by an elastic beam.	44
Figure 3.1.	Rectangular plate simply supported on two edges.	49
Figure 3.2.	Convergence of maximum deflection (Δ_{max}) in a rectangular plate with two edges simply supported and two edges free.	52
Figure 3.3.	Convergence of maximum bending moments $(M_x)_{max}$ and $(M_y)_{max}$ in a rectangular plate with two edges simply supported and two edges free.	55
Figure 3.4.	Comparison of maximum bending moment $(M_x)_{max}$ for different numbers of strips used to discretize the plate.	57
Figure 3.5.	Comparison of maximum bending moment $(M_y)_{max}$ for different numbers of strips used to discretize the plate.	58
Figure 3.6.	Square plate simply supported on two edges with the other two edges supported by elastic beams.	59

FIGURE PAGE

Figure 3.7. Convergence of maximum deflection (Δ_{max}) in a square plate with two edges simply supported and two edges supported with elastic beams. 61

Figure 3.8. Convergence of maximum bending moment $(M_x)_{max}$ in a square plate with two edges simply supported and two edges supported with elastic beams. 62

Figure 3.9. Convergence of maximum bending moment $(M_y)_{max}$ in a square plate with two edges simply supported and two edges supported with elastic beams. 63

Figure 3.10. Simply supported single strip with a centrally located beam. 64

Figure 3.11. Comparison between the finite strip method and elastic beam theory for deflection, moment and shear in a beam. 66

Figure 3.12. Fourier series approximations at a point of discontinuity in beam shear. 67

Figure 4.1. Single Span Composite Bridge. 70

Figure 4.2. Truck Positioning for a Single-lane Loading Case. 71

Figure 4.3. Effects of Slab Thickness on Distribution Factors for Moment. 73

Figure 4.4. Effects of Span Length on Maximum Distribution Factor for Moment. 74

Figure 4.5. Comparison of Maximum Distribution Factors for Moment for the Single-lane Loading Case. 76

Figure 4.6. Truck Positioning for a Multi-lane Loading Case. 77

Figure 4.7. Comparison of Maximum Distribution Factors for Moment for the Multi-lane Loading Case. 78

Figure 4.8. Effects of Girder Spacing on Maximum Distribution Factors for Moment. 79

Figure 4.9. Effects of Girder Spacing on Maximum Distribution Factors for Shear. 80

Figure 4.10. Axle Configuration and Load Distribution for an MX Transporter. 81

Figure 4.11. Distribution Factors for Moment and Shear for an MX Transporter. 83

Figure A.1. Sequence of operations in the finite strip computer algorithm. 91

LIST OF TABLES

TABLE PAGE

Table 3.1. Maximum plate actions as a function of beam flexural rigidity. 60

LIST OF APPENDICES

APPENDIX PAGE

Appendix A COMPUTER ALGORITHM. 90

Appendix B BRASS-DISTRIBUTION FACTOR DOCUMENTATION 92

CHAPTER 1

INTRODUCTION

1.1. GENERAL

For over sixty years the American Association of State Highway and Transportation Officials (AASHTO) has published standard specifications for bridge design. Throughout the years several studies have been devoted to the distribution of wheel loads on highway bridges. As the results of these studies became available, modified provisions were developed for the specification. Unfortunately, this process has caused a nonuniformity in the specification's design criteria, and in some cases even conflicting design parameters (*20*). It has been determined that the AASHTO specifications for highway bridges (*Standard Specifications for Highway Bridges*, 1989) can result in overly conservative designs, which can be directly attributed to it's simplistic wheel load distribution factors (*5*).

There is an obvious need to improve the criteria for the distribution of wheel loads on highway bridges. In 1985 the National Cooperative Highway Research Program (NCHRP) undertook a comprehensive study to consolidate, update, and improve the criteria for wheel load distribution. The study was completed in 1991 and the results

were presented in NCHRP Project 12–26, *Distribution of Wheel Loads on Highway Bridges*, by Imbsen and Associates, Inc. As a result of this research, a draft specification was prepared for determining of wheel load distribution factors, and was recommended as a replacement for the current AASHTO specifications for highway bridges.

In the past few years there have been several developments for simplified methods of determining the load distribution characteristics of highway bridges. Some of these developments have been in defining the behavior of a bridge with a minimum number of dimensionless characterizing parameters. Other developments have concentrated on using a finite element approach and performing a series of parameter studies to try to develop a simplified formula for determining distribution factors. Although a great deal of research has been devoted to this topic, practicing U. S. engineers today are using the simplified AASHTO method. It should be noted that the use of more complex methods has always been an option in the AASHTO specifications, but is rarely exercised.

1.2. PRINCIPLES OF TRANSVERSE LOAD DISTRIBUTION

The distribution of transverse loads in highway bridges is difficult to quantify. The load distribution in a bridge is a function of the magnitude and location of the loads and the response of the bridge to these loads (*12*). A portion of the load goes into the bending of the bridge deck, and the remaining load is distributed to the girders per their relative rigidities, span and spacing. The problem now becomes determining how these transverse loads are distributed to the individual girders.

To visualize how the transverse load distribution varies along the span, a few simple examples from Bakht and Moses (5) are used. The first example is a simple grillage analysis of three longitudinal beams connected by a transverse beam at midspan. The system is loaded with a point load P at midspan as shown in Figure 1.1.

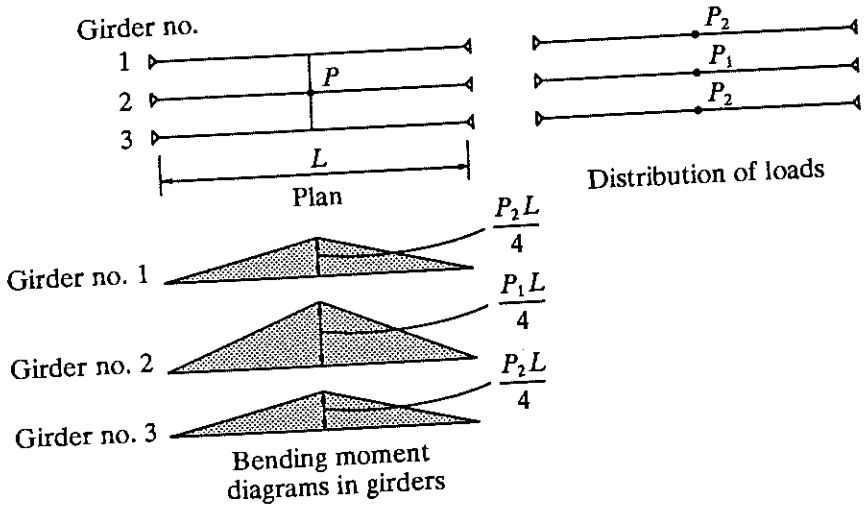

Figure 1.1. Load Distribution in Girders Connected by One Transverse Beam (from Bakht and Moses (5)).

If the transverse beam was not present, the entire load P would be carried by the interior girder causing a maximum bending moment of $PL/4$, and the resulting moment diagram would be referred to as the "free" moment diagram (5). Due to the transverse beam, some of the load P distributes to the other two girders in proportion to their relative stiffnesses. Notice in Figure 1.1 that

> *The bending moment diagram for any beam can be obtained by multiplying the free moment diagram with a scalar quantity. This scalar quantity which gives a measure of load distribution between the longitudinal beams, is also referred to as the distribution factor (DF).* (5)

For the second example, two additional transverse beams are added making a total of three connecting beams as shown in Figure 1.2. For demonstration purposes, the torsional stiffness of the connection beams is neglected. Notice in Figure 1.2 that by including the additional transverse beams, the shape of the bending moment diagrams drastically changes from the first example with only one transverse beam. In comparing the two sets of moment diagrams in Figure 1.2, it can be shown that the fraction of the free moment diagram, or distribution factor, for any one of the girders varies along the span (*5*).

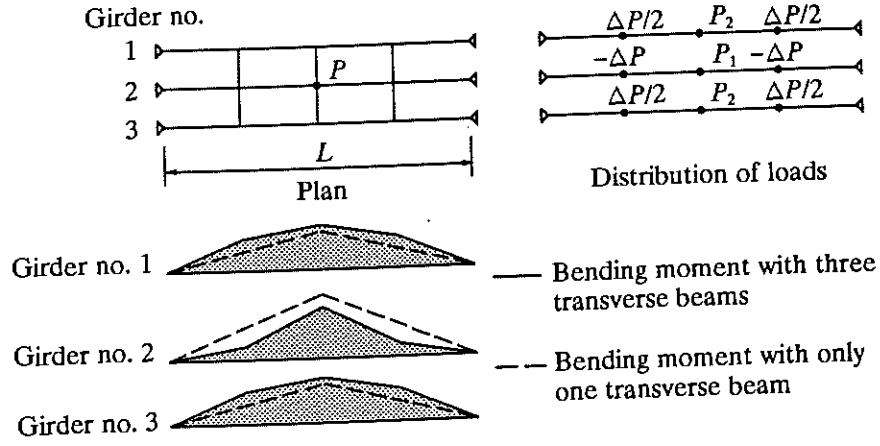

Figure 1.2. Load Distribution in Girders Connected by Three Transverse Beams (from Bakht and Moses (*5*)).

In an actual highway bridge, the bridge deck responds similar to an orthotropic plate. Conceptually this would be similar to an infinite number of transverse beams connecting the girders. In fact, it has been shown by Bakht and Moses (*5*) that for this situation, the shape of the bending moment diagrams take the form shown in Figure 1.3. In real life cases, the girders are seldom directly loaded, and more often there are several loads along the span, which further complicates the analysis.

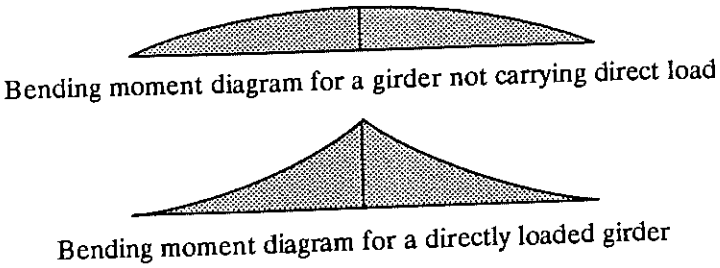

Figure 1.3. Shape of Bending Moment Diagrams (from Bakht and Moses (5)).

It should be noted that while the distribution factor has been defined in terms of bending moment, it can also be defined in terms of beam shear. In fact, a comparison between distribution factors for both shear and moment is presented as part of this investigation.

1.3. TRUCK LOADS ON HIGHWAY BRIDGES

There are several different types of loads that a highway bridge must sustain, and the distribution process for each type of load is different. Always present is the selfweight of the bridge, known as the dead load. Providing that the girders have the same material and sectional properties, the structure dead load is assumed to distribute equally among the girders. This makes the analysis process relatively simple for dead load. The live loads, or truck loads, are of complex nature, and the distribution of these live loads is the focus of this study.

1.3.1. STANDARD TRUCK LOADS

The American Association of State Highway and Transportation Officials (AASHTO) *Standard Specifications for Highway Bridges* has several different classes of truck loading. Section 3.7.2 states that

There are four standard classes of highway loading: H 20, H 15, HS 20 and HS 15. Loading H 15 is 75 percent of loading H 20. Loading HS 15 is 75 percent of loading HS 20. If loadings other than those designated are desired, they shall be obtained by proportionately changing the weights shown for both the standard truck and the corresponding lane loads. (22)

An example of the HS designation is presented in Figure 1.4. The specification also states that, "For truck highways, or for other highways that carry, or may carry, heavy truck traffic, the minimum live load shall be the HS 15 designated herein." (22)

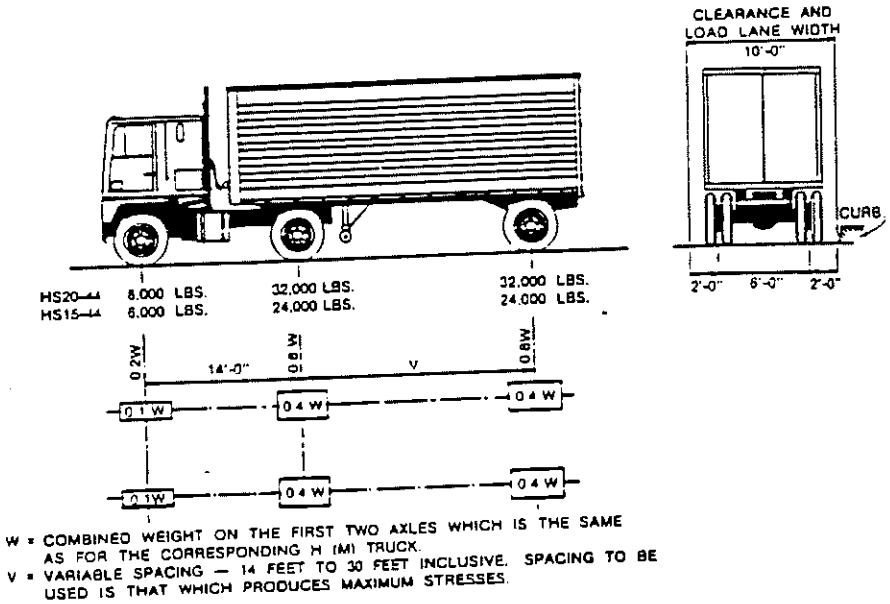

Figure 1.4. **Standard AASHTO HS Truck (Figure 3.7.7A from AASHTO *Standard Specifications for Highway Bridges*, 13th Edition (1989)).**

1.3.2. PERMIT VEHICLE LOADS

State authorities place limits on both the size and weight of motor vehicles that operate on the highway systems within a state. When a motor vehicle is transporting an indivisible piece of cargo that exceeds the specified limits in height, length, width or weight,

a permit must be obtained before shipping begins. Typical shipments that require a permit include mobile homes, construction equipment and large electrical transformers, to name a few. An example of a permit type vehicle is shown below in Figure 1.5.

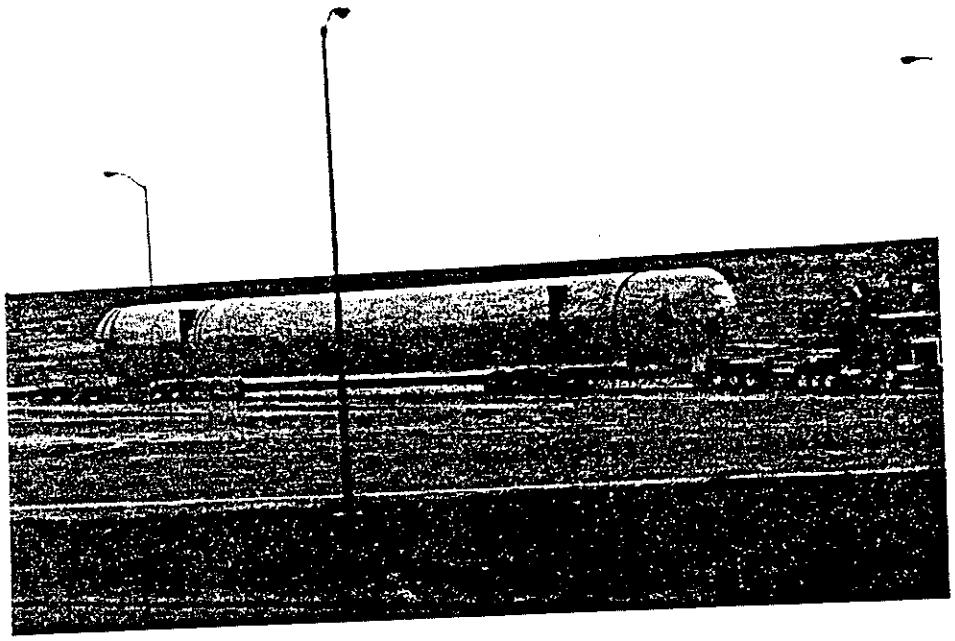

Figure 1.5. Permit Vehicle with an indivisible piece of cargo.

The primary objective of the use of permits is to control shipments of cargo that exceed specified limits and cargo that cannot be readily dismantled. This is done to protect the structural integrity of the highway system and prevent such shipments from creating traffic safety hazards or delays to other motorists (*10*).

Many states designate a specific route that a permit vehicle must take on the highway system. These routes are determined by geometric characteristics of the highway, such as overhead structures and lane widths, and also the structural capacity of the bridges. In fact some states issue a route map with the permit to specify in written terms the route that must be followed.

There are several different types of overlimits for which a permit is granted. An individual shipment may be overweight, oversize or both. An oversize load could be overwidth, overlength, overheight, or any combination of the three. An overweight load, or overload, typically refers to the gross overweight of the vehicle or the overweight of it's individual axles. An example of an overload vehicle is shown in Figure 1.6. This particular photograph was taken by the Wyoming Highway Patrol at the port of entry in Cheyenne, Wyoming. Notice that there are eight wheels through each axle to distribute the load over a larger area.

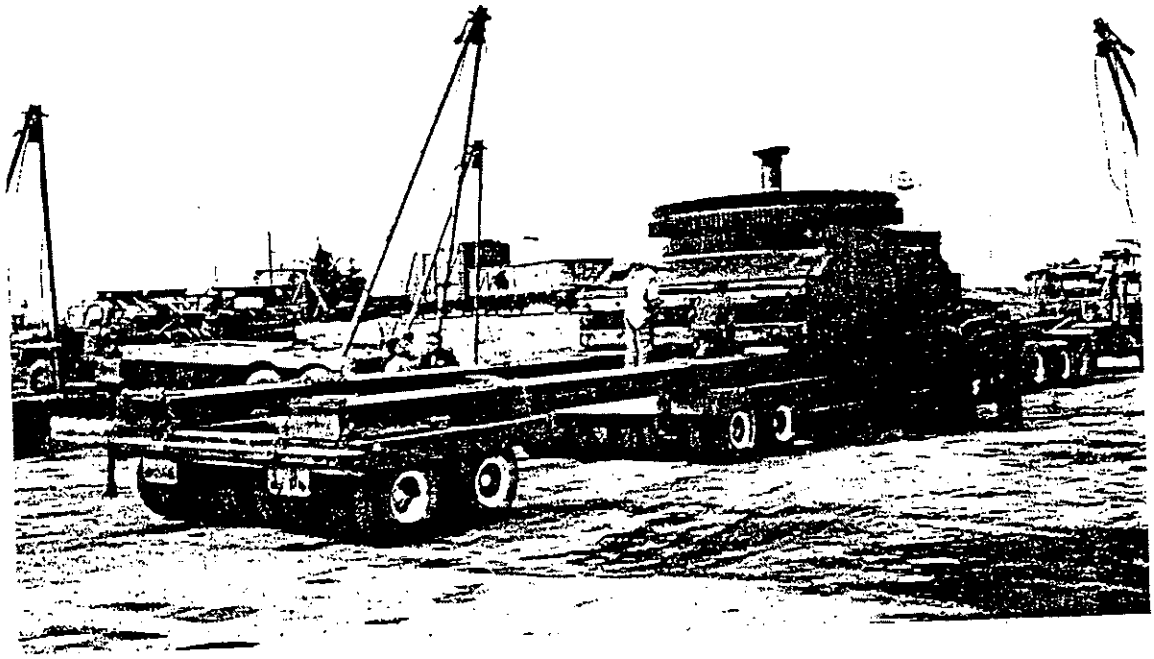

Figure 1.6. Overweight Permit Vehicle.

These overload vehicles are of critical importance both in the design of new bridges and in the evaluation of the capacity of existing bridges. The AASHTO *Standard Specifications for Highway Bridges* has special provisions for overload vehicles. Article 3.5.1 states that

> *...the live load* [is] *assumed to occupy a single lane without concurrent loading in any other lane. The overload shall apply to all parts of the structure affected, except the roadway deck, or roadway deck plate and stiffening ribs in the case of orthotropic bridge superstructures.* (*22*)

1.4. REVIEW OF CURRENT LITERATURE

There is an enormous amount of literature devoted to the distribution of transverse loads on highway bridges. It is not the authors' intent to review all of the available literature on this topic. The literature review is limited to the available simplified methods of determining distribution factors for slab–on–girder type bridges. For reasons that will become obvious later, only simply supported bridges are considered. Bridges with skewed supports on curved alignments and/or continuous over interior supports are outside the scope of this study. Other types of bridges, such as box girder bridges, slab bridges, multi–box beam bridges or spread box–beam bridges, were not studied in this research. Special bridge types like truss, arch and cable supported bridges, were also excluded.

1.4.1. AASHTO METHOD

Distribution factors allow engineers to analyze the response of a bridge by treating the longitudinal and transverse effects of wheel loads as uncoupled phenomena (*12*). Empirical distribution factors for the girders of a bridge present in the AASHTO *Standard Specifications for Highway Bridges* have remained relatively unchanged since the first publication in 1931 (*12*). The specifications reflected the state of the art at that time.

The current AASHTO specifications allow for simplified analysis of bridges utilizing the concept of a wheel load distribution factor for bending moment and shear in the interior girders of common types of bridges (*12*). By using this simplified method of load distribution,

the complex analysis of a bridge subjected to one or more vehicles is reduced to "the simple analysis of a beam." (5) Using this method, the maximum load effects in a girder are obtained by assuming the girder to be a one-dimensional beam subjected to a load obtained by multiplying one line of wheels of the design vehicle by a distribution factor *(DF)*. This distribution factor is given by

$$DF = \frac{S}{D} \qquad \ldots\ldots\ldots\ldots\ldots\ldots\ldots\ldots\ldots\ldots (1.1)$$

where S is the center-to-center spacing of the girders, and D is a constant that varies with bridge type, geometry and number of lanes of traffic. The original concept of the D factor was developed by Newmark (*16*) in 1948 for use in the design of I-beam bridges. Once the value of D has been selected for the bridge, the maximum moments in a girder can be obtained from equation (1.2).

$$M_{girder} = \left(\frac{S}{D}\right) M \qquad \ldots\ldots\ldots\ldots\ldots\ldots\ldots\ldots\ldots\ldots (1.2)$$

where M is the moment determined from a beam analysis of the loads assumed to act directly on the girder, and D carries the units of length.

AASHTO gives several values of D for various types of bridge decks and supporting elements. Specifically, it states that, "In the case of a span with concrete floor supported by 4 or more steel stringers, the fraction of the wheel load shall not be less than:" (*22*)

$$DF = \frac{S}{5.5}$$

This applies to a bridge designed for two or more lanes of traffic. For a bridge designed for a single traffic lane, or one lane loaded, the distribution factor should not be less than

$$DF = \frac{S}{7.0}$$

While the current AASHTO method benefits from its simplicity of use, it has been established that this method is too simple and cannot take into account all of the aspects of a bridge that influence its load distribution characteristics. The National Cooperative Highway Research Program (NCHRP) has identified several shortcomings of the current AASHTO method of load distribution. Some of them are:

- It Considers only a limited number of factors affecting distribution.
- It doesn't uniformity in consideration of reduction in load intensity for multiple lane loading.
- It has variation in format for bridges of similar construction.

1.4.2. NCHRP PROJECT 12–26

In 1985 the Transportation Research Board undertook a comprehensive study to consolidate, update and improve the criteria for wheel load distribution. The study was completed in 1991 and the results were presented in NCHRP Project 12–26. The primary objective of this study was to develop comprehensive specifications for distribution of wheel loads on highway bridges.

The research focused on the more commonly used bridge types such as beam and slab bridges, box girder bridges, slab bridges, multi–box beam bridges and spread box beam bridges (*12*). Three alternative levels of analysis were considered for each type of bridge.

Level one analysis included simplified formulae for predicting the distribution of transverse loads. These formulae were developed for determining the distribution factors for shear and moment in interior and exterior girders for single or multiple lane loading (*12*). These formulae were based on the standard AASHTO HS family of trucks. Level two included either graphical methods, influence surfaces, or a plane grillage analysis. Level three involved a detailed finite element model of both the bridge deck and the supporting elements. This was accomplished through the use of production finite element modeling software, such as FINITE (*11*) and SAP (*1*).

An important part in developing the simplified methods used in the level one analysis was compilating a database of actual bridges. Bridges from various state departments of transportation were selected at random to achieve a national representation (*12*). The database included several bridges types: 365 beam and slab bridges, 112 prestressed concrete bridges, 121 reinforced concrete box girder bridges, 130 slab bridges, 67 multi-box beam bridges, and 55 spread box beam bridges (*12*). The database was studied to identify common values of parameters that influence a bridges load distribution characteristics. For each bridge type, a hypothetical bridge was created that possesses the average properties of the bridges of that type.

In order to determine the effect of the bridge parameters on load distribution, each parameter in the average bridge was varied one at a time. The variation of distribution factors with each parameter established the importance of each parameter (*12*). The simplified formulae were developed to capture the variation in distribution factors with each identified parameter (*12*).

In the development of the simplified formulae it was assumed that the effect of each parameter could be modeled with an exponential function of the form ax^b, where x is the value of the individual parameter, and a and b are constants that represent the variation in x. It was also assumed that parameters are independent of each other, allowing each parameter to be considered separately (*12*).

The distribution factor g was modeled with an exponential formula of the form $g=(a)(S^{b1})(L^{b2})(t^{b3})(...)$ where a is a scale factor, S, L and t represent girder spacing, span length and deck thickness, respectively, and $b1$, $b2$ and $b3$ are constants that represent the nonlinearity in S, L and t, respectively (*12*). The procedure for determining the values of a, $b1$, $b2$ and $b3$ in the simplified formula was: Assume that, for only two cases, all of the bridge parameters are the same except S, then NCHRP (*12*) states that

$$g_1 = (a)\left(S_1^{b1}\right)\left(L^{b2}\right)\left(t^{b3}\right)(\ldots)$$
$$g_2 = (a)\left(S_2^{b1}\right)\left(L^{b2}\right)\left(t^{b3}\right)(\ldots)$$

therefore,

$$\frac{g_1}{g_2} = \left(\frac{S_1}{S_2}\right)^{b1}$$

or

$$b_1 = \frac{\ln \frac{g_1}{g_2}}{\ln \frac{S_1}{S_2}}$$

If n different values of S are examined and successive pairs are used to determine the value of b1, then (n–1) different values for b1 can be obtained. If these b1 values are close to each other, an exponential curve may be used to accurately model the variation of the distribution factor with S. (*12*)

Once all of the factors $b1, b2, b3$, etc. were determined, the value of the scale factor a for the average bridge was obtained by

$$a = \frac{g_0}{\left(S_0^{b1}\right)\left(L_0^{b2}\right)\left(t_0^{b3}\right)(\ldots)}$$

Once the simplified formulae were derived, they were then applied to the bridges in the database for which they were intended. These bridges were also analyzed with either a level two or level three analysis to verify the accuracy of the formulae. The distribution factors obtained by the more accurate analysis were compared to values obtained from the simplified methods (*12*). A ratio of approximate to accurate distribution factors was examined to assess the accuracy of the simplified method (*12*). The standard deviation was determined for each formula, and the method or formula with the smallest standard deviation was considered the most accurate (*12*).

The following equations are the result of the extensive research performed in NCHRP project 12–26. These equations were developed for determining the distribution factors for shear and moment in interior and exterior girders of slab girder bridges with single or multiple lane loading (*12*). The equations include the effects of girder spacing, span length, girder inertia, and slab thickness.

The distribution factor for moment in the interior girders of slab–girder bridges subjected to multiple lane loading is given by

$$g_{SG\text{-}M} = 0.15 + \left(\frac{S}{3}\right)^{0.6}\left(\frac{S}{L}\right)^{0.2}\left(\frac{K_g}{Lt_s^3}\right)^{0.1} \quad \ldots\ldots\ldots\ldots\ldots\ldots (1.3)$$

where

S = girder spacing $(3.5' \le S \le 16')$

L = span length $(20' \le L \le 200')$

t_s = slab thickness $(4.4'' \le t_s \le 12'')$

K_g = $n(I + Ae^2)$ $(1\text{x}10^4 \le K_g \le 7\text{x}10^6\ \text{in}^4)$

where

n = modular ratio of girder material to slab material, dimensionless

I = girder moment of inertia, in^4

A = girder cross sectional area, in^2

e = girder eccentricity, distance from girder centroid to midpoint of slab, in.

A correction factor for edge girders, to be multiplied by the distribution factor for interior girders in equation (1.3) is given by

$$e_{SG\text{-}M} = \frac{7 + d_e}{9.1} \ge 1.0 \quad \ldots\ldots\ldots\ldots\ldots\ldots (1.4)$$

where

d_e = distance in feet from center of the exterior girder to the edge of the exterior lane. If the edge of the lane is outside of the exterior girder, the distance is positive; and if the edge of the lane is to the interior side of the girder, the distance is negative.

The distribution factor for moment in the interior girders of slab–girder bridges subjected to single lane loading is given by

$$g_{SG\text{-}M1} = 0.1 + \left(\frac{S}{4}\right)^{0.4}\left(\frac{S}{L}\right)^{0.3}\left(\frac{K_g}{Lt_s^3}\right)^{0.1} \quad \ldots\ldots\ldots\ldots\ldots\ldots (1.5)$$

It was recommended that simple beam distribution in the transverse direction be used to determine the distribution of moment to edge girders in the single lane loading case.

The distribution factor for shear in the interior girders of slab–girder bridges subjected to multiple lane loading is given by

$$g_{SG\text{-}V} = 0.4 + \left(\frac{S}{6}\right) - \left(\frac{S}{25}\right)^2 \quad \ldots\ldots\ldots\ldots\ldots\ldots\ldots\ldots (1.6)$$

A correction factor for edge girders, to be multiplied by the distribution factor for interior girders in equation (1.6) is given by

$$e_{SG\text{-}V} = \frac{6 + d_e}{10} \quad \ldots\ldots\ldots\ldots\ldots\ldots\ldots\ldots (1.7)$$

The distribution factor for shear in the interior girders of slab–girder bridges subjected to single lane loading is given by

$$g_{SG\text{-}V1} = 0.6 + \left(\frac{S}{15}\right) \quad \ldots\ldots\ldots\ldots\ldots\ldots\ldots\ldots (1.8)$$

It was also recommended that simple beam distribution in the transverse direction be used to determine the distribution of shear to edge girders in the single lane loading case.

1.4.3. ONTARIO HIGHWAY BRIDGE DESIGN CODE

The Ontario Highway Bridge Design Code (*17*) was the first comprehensive bridge design code developed in recent years (*20*). The second edition, published in 1983, made extensive use of the latest available technology and research, and was also the first to incorporate a limit–state design for bridges in which possible modes of failure are identified (*20*).

In the Ontario code the method for determining the distribution of loads was developed in part by Baider Bakht (*2*). The method was developed to include such effects as bridge width, girder spacing, number of loaded lanes, bridge span, and strength properties of bridge components (*20*).

In the development of the simplified method, a small number of dimensionless parameters were used to characterize the behavior of a bridge (*5*). It was assumed that the load distribution in a bridge could be modeled by a simply supported rectangular orthotropic plate. The two characterizing parameters needed to define the behavior of the plate are given by Bakht and Moses (*5*). The two parameters α and θ are given by

$$a = \frac{D_{xy} + D_{yx} + D_1 + D_2}{2(D_x D_y)^{0.5}} \quad \ldots\ldots\ldots\ldots\ldots\ldots\ldots (1.9)$$

$$\theta = \frac{b}{L}\left(\frac{D_x}{D_y}\right)^{0.25} \quad \ldots\ldots\ldots\ldots\ldots\ldots\ldots\ldots (1.10)$$

where

x = the longitudinal direction
y = the transverse direction
b = half width of the plate
L = span of the plate
D_x = the longitudinal flexural rigidity per unit width
D_y = the transverse flexural rigidity per unit length
D_{xy} = the longitudinal torsional rigidity per unit width
D_{yx} = the transverse torsional rigidity per unit length
D_1 = the longitudinal coupling rigidity per unit width
D_2 = the transverse coupling rigidity per unit length

A third characterizing parameter was used to represent edge stiffening in the plate, It was assumed that the effects of edge stiffening could by represented by the parameter λ given by

$$\lambda = \frac{EI}{L}\left(\frac{1}{D_x^3 D_y}\right)^{0.25} \qquad \ldots\ldots\ldots\ldots\ldots\ldots\ldots\ldots (1.11)$$

where EI is the flexural rigidity of an individual edge beam.

The current Ontario Highway Bridge Design Code (*17*) employs a semi-graphical technique for determining distribution factors. The graphical technique was originally proposed by Bakht and Jaeger (*4*). The method required the calculation of the parameters α, θ and λ. Numerical values for D and C_f are read from appropriate charts, and are then used in equation (1.12). A typical set of design charts is shown in Figure 1.7.

These charts have been developed for several different numbers of traffic lanes. Once the appropriate values for D and C_f have been determined, the design value of D (D_d), which is analogous to the value of D used in the AASHTO method, is determined for each of the internal and external girders by equation (1.12).

To account for the presence of edge stiffening, equation (1.12) is modified by a factor C_e that is obtained from the appropriate chart with the value of λ. This modified equation is given by

$$D_d = D\left(1 + \frac{\mu C_f + C_e}{100}\right) \qquad \ldots\ldots\ldots\ldots\ldots\ldots\ldots\ldots (1.13)$$

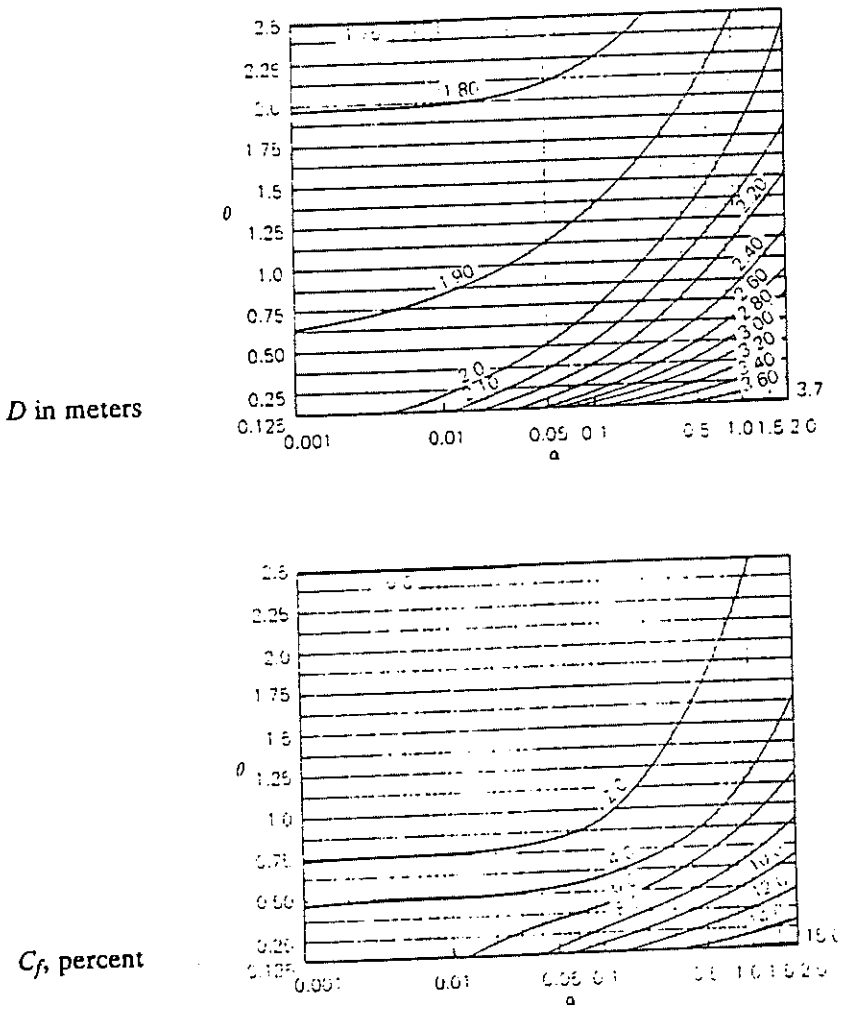

Figure 1.7. **Design charts for determining values of D and C_f for a two lane bridge (reproduced from *Ontario Highway Bridge Design Code (1983)*).**

The method employed by the Ontario code was verified by comparing the results to those obtained from both finite element analyses and field testing. The majority of the verification was performed as part of the research used in NCHRP project 12-26. The same database that was compiled for the NCHRP project was used to verify the current method used in Ontario code.

$$D_d = D\left(1 + \frac{\mu C_f}{100}\right) \quad \text{.....(1.12)}$$

where

$\mu = \frac{W_e - 11}{2}$ for U.S. customary units

$\mu = \frac{W_e - 3.3}{0.6}$ for metric units

W_e = the design lane width in feet for U.S. customary units and in meters for metric units.

1.4.4. OTHER METHODS

In addition to the simplified methods used today in practice, there are several other methods to determine the distribution of loads on highway bridges. Limiting the discussion to slab and girder bridges, Marx, et al (*15*), at the University of Illinois developed a simplified formula for determining the distribution factor for moment in the interior girders of a multi-lane loaded bridge (*12*). This equation is

$$g = \left(\frac{S}{Q}\right) \quad \text{.....(1.14)}$$

where

S = girder spacing, ft.

$Q = \left(0.01538 + \frac{S}{150}\right)\left(\frac{L}{H^{0.5}}\right) + 4.26 + \frac{S}{30}$

where

L = span length, ft.

H = bridge stiffness ratio $= \frac{E_g I_g}{LD}$

where

E_g = girder modulus of elasticity, ksi.

I_g = girder moment of interia, in^4.

D = flexural slab stiffness parameter $= \frac{E_s t_s^3}{12(1-\nu^2)}$

where

E_s = slab modulus of elasticity, ksi.

t_s = slab thickness, in.

ν = Poisson's ratio of the slab, dimensionless.

In addition to equation (1.14) a formula was also developed for determining the distribution

factor for moment in the exterior girders of a multi-lane loaded bridge. This equation is

$$g = \left(\frac{S}{Q}\right) \quad \ldots\ldots\ldots\ldots\ldots\ldots\ldots\ldots\ldots\ldots (1.15)$$

where

$$Q = 400H\left(\frac{S}{L}\right)^3 - 478\left[H\left(\frac{S}{L}\right)^3\right]^{1.1} + 6.7 \quad \text{for } H\left(\frac{S}{L}\right)^3 < 0.0569$$

$$Q = 5.24H\left(\frac{S}{L}\right)^3 + 8.74 \quad \text{for } H\left(\frac{S}{L}\right)^3 \geq 0.0569$$

The parameters are same as those for equation (1.14).

Another formula for determining the distribution factor for moment in the interior girders of a single-lane loaded bridge was developed at Lehigh University (*26*). This equation is

$$g = \left(\frac{2N_1}{N_b}\right) + k_1\left(\frac{S}{L}\right)^{\frac{1}{3}} \quad \ldots\ldots\ldots\ldots\ldots\ldots\ldots\ldots\ldots\ldots (1.16)$$

where

$$k_1 = \frac{1}{9}\left(\frac{W_c}{N_b}\right)\left(\frac{W_c}{12N_1}\right)^{\frac{3}{2}}$$

N_1 = number of design traffic lanes
N_b = number of beams $(3 \leq N_b \leq 17)$
S = girder spacing $(3' \leq S \leq 11')$
L = span length $(30' \leq L \leq 135')$
W_c = roadway width between curbs $(24' \leq W_c \leq 72')$

As part of an early report presented by the National Cooperative Highway Research Program, Sanders and Elleby (*21*) developed a formula based on orthotropic plate theory for determining distribution factors for moment in the interior girders of a multi-lane loaded bridge (*12*). This equation is given by

$$g = \left(\frac{S}{D}\right) \quad \text{.....(1.17)}$$

where

S = girder spacing

$$D = 5 + \left(\frac{N_1}{10}\right) + \left(\frac{3 - 2N_1}{7}\right)\left(\frac{1 - C}{3}\right)^2 \quad \text{for } C \leq 3$$

$$= 5 + \left(\frac{N_1}{10}\right) \quad \text{for } C > 3$$

where

S = girder spacing
N_1 = total number of design traffic lanes
C = a stiffness parameter that depends on type of bridge, bridge and beam geometry, and material properties.

While not considered a simplified method, the finite element method is a viable solution for determining the distribution of loads on highway bridges. This method was employed by Tarhini and Frederick (*23*). In the development of the simplified formula, a three–dimensional finite element analysis was used to model the behavior of a typical slab–on–girder bridge. The concrete deck was modeled with an isotopic eight–noded brick element (*23*). Both the flanges and the webs of the girders were modeled with three–dimensional, four–noded, quadrilateral plate elements capable of simulating in–plane and out–of–plane deformation (*23*). The finite element models were generated with standard AASHTO HS 20 truck loadings (*23*).

Several parameters were varied in the modeling process, including the number of girders, the span length and the number and positioning of the trucks. Finite element modeling and post processing were performed with ICES STRUDL II (*13*). The maximum wheel load distribution factors were determined from the finite element analyses by the following equation (*23*).

$$(DF)_{max} = \frac{(M_{FEA})_{max}}{(M_{girder})_{max}} \quad \ldots\ldots\ldots\ldots\ldots\ldots\ldots\ldots\ldots\ldots (1.18)$$

where $(M_{FEA})_{max}$ is the maximum moment in the girder as determined from the finite element analysis, and $(M_{girder})_{max}$ is the maximum moment in the girder as determined from a single beam subjected to one line of wheels (typically half the axle weight). A wheel load distribution formula relating span length and girder spacing was developed from the finite element analyses (*23*). The formula is

$$DF = 0.00013L^2 - 0.021L + 1.25\sqrt{S} - \frac{(S+7)}{10} \quad \ldots\ldots\ldots\ldots\ldots\ldots (1.19)$$

where L is the bridge span length (ft.) and S is the girder spacing (ft.).

The results obtained from this simplified formula were compared to both the AASHTO and Ontario methods. These results were also compared to a scale model bridge in which strain gages were mounted on both the concrete deck and the steel girders. It was determined that the maximum experimental distribution factors were 1.04 for exterior girders and 1.19 for interior girders (*23*). The AASHTO method predicted values of 1.28 and 1.36 for exterior and interior girders, respectively, and equation (1.19) predicted 1.18 (*23*).

1.5. OBJECTIVES AND SCOPE

There are two main objectives of the research described here. The first objective is to develop an automated procedure for determining the distribution factors for both moment and shear in the girders of slab–on–girder highway bridges subjected to both standard truck loading and permit vehicle loading. The second objective is to evaluate the current simplified

methods for determining the distribution of loads on highway bridges. Further, these methods are compared to the automated approach to demonstrate the degree of conservatism of such simplified methods.

The scope of this investigation is limited to simply supported slab–on–girder bridges. Only bridges that are rectangular in plan are considered. The effects of skewed supports on curved alignments and/or continuous over interior supports are outside the scope of this study.

CHAPTER 2

GENERAL THEORY AND FORMULATION OF THE FINITE STRIP METHOD

2.1. INTRODUCTION

Many of today's civil engineering structures fall into the category of flat plate systems. An excellent example of a flat plate system is a bridge deck. Traditionally, the analysis of what are termed "thin plates" is based on Kirchoff assumptions (*24*), which require solving a nonhomogeneous biharmonic differential equation with the appropriate boundary conditions (*19*). Classical solutions to thin plate problems are limited to a few relatively simple types.

A contemporary approach to solving these types of flat plate systems is the finite element method (FEM) (*1,27*). However, in order to obtain an accurate model with the FEM, a relatively fine mesh is required, which involves solving a large number of simultaneous equations. Further, the storage and computational time required for an accurate FEM analysis of a large plate system can be exceedingly large compared to the available storage capacity of some computers (especially microcomputers).

In addition, the versatility of the FEM is not required for flat plate systems with regular geometry and continuous boundary conditions. A methodology developed by Cheung (*8*), termed the "finite strip method," is better suited for these types of flat plate systems. Because the plan geometry of the plate is discretized in one principal direction only, the finite strip method considerably reduces the number of equations to be solved (*19*).

The finite strip method can be considered a special form of the finite element method using the displacement approach. The primary difference between the two methods is that the FEM uses polynomial displacement functions in all directions, and model refinement is obtained by increasing the number of elements in all directions, while the FSM uses simple polynomials in some directions and continuously differentiable smooth series in the other directions. The series displacement functions are more accurate than the polynomial displacement functions, therefore model refinement is obtained by increasing the number of elements in the polynomial direction only. One stipulation to the method is that the series should satisfy *a priori* the boundary conditions at the ends of the strips (*8*). Essentially the FSM reduces a two-dimensional analysis to a series of one-dimensional analyses. The general form of the displacement function is given as a product of simple polynomials and series:

$$w(x,y) = \sum_{m=1}^{r} f_m(x) Y_m \qquad \ldots\ldots\ldots\ldots\ldots\ldots\ldots\ldots (2.1)$$

As stated previously, the finite strip method discretizes the continuum in one direction only. A procedure for the FSM originally developed by Cheung (*8*) is given as:

(i) The continuum is divided into a finite number of strips via imaginary lines called "nodal lines". The ends of each strip coincide with actual boundaries of the continuum (Figure 2.1).

(ii) Each strip is assumed to be connected with each adjacent strip by nodal lines which also define longitudinal boundaries of the strips. The degrees of freedom (DOF) for the strip are assumed to occur at each nodal line. These DOF are referred to as the nodal displacement parameters.

(iii) Both the displacement field and stress and strain fields for each element are represented with a displacement function in terms of the nodal displacement parameters.

(iv) Once the displacement function is chosen, and the loads acting on the strip are known, strip stiffness and load matrices can be obtained from principles of virtual work or minimum total potential energy.

(v) The individual strip stiffness and load matrices are then assembled into a set of system stiffness equations. These equations are then solved with typical matrix techniques to yield the nodal displacement parameters.

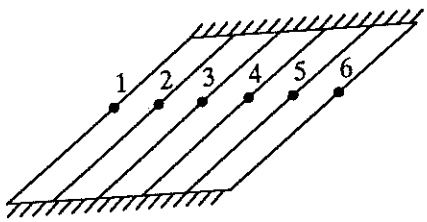

Figure 2.1. Discretization of a continuum into a finite number of strips.

2.2. CHOICE OF DISPLACEMENT FUNCTIONS

The displacement functions used in the finite strip method are a combination of hermitian polynomials in the transverse (x) direction and continuously differentiable smooth series in the longitudinal (y) direction, as shown in Figure 2.2. The choice of displacement functions for an individual strip is one of the most crucial parts of the analysis (*8*). A poorly chosen displacement function may result in erroneous nodal displacement parameters, otherwise known as degrees of freedom. Further, the results of the analysis might converge to the wrong answer for successively refined meshes (*8*).

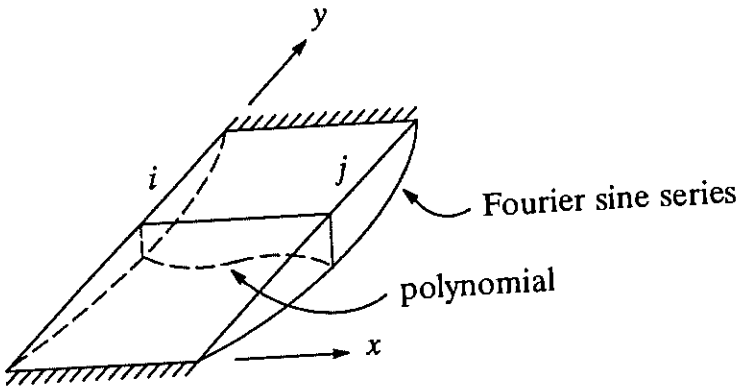

Figure 2.2. Typical finite strip with simple support conditions.

One way to ensure convergence to the correct answer is to place the following restrictions on the displacement functions.

(i) As a stipulation of the finite strip method stated previously, the series part (Y_m) of the displacement function must satisfy *a priori* the boundary conditions at the ends of the strips.

(ii) The polynomial part ($f_m(x)$) of the displacement function must be able to represent a state of constant strain in the x direction.

The second condition, a state of constant strain, can be satisfied in the following manner.

The polynomial part of the displacement function ($f_m(x)$) takes the form $A + Bx + Cx^2 + ...$ "...constant strain will exist if the polynomial is complete up to or above the order in which a constant term will actually be obtained when the necessary differentiation for computing strains are carried out." (*8*)

Each part of the displacement function (Equation 2.1), the polynomial part ($f_m(x)$), and the series part (Y_m), is discused separately for convenience.

2.2.1. SHAPE FUNCTION PART OF DISPLACEMENT FUNCTION

Before an appropriate displacement function can be assumed for a strip, the characteristics of the actual deformed surface should be taken into account. For simplicity, the simply supported flat plate system will be considered, and how to incorporate different boundary conditions is shown later. As a result of the simple support conditions, the displacement function must produce zero deflections at the supports. Further, the bending moments in the longitudinal direction must also equal zero at the two end supports. From Figure 2.2, it is apparent that a transverse (x) section of the deflected surface can be simulated by joining a number of polynomial functions.

The assumed displacement function for a strip now takes the form

$$w(x,y) = \sum_{m=1}^{r} f_m(x)Y_m = \sum_{m=1}^{r} (A + Bx + Cx^2 + Dx^3 + ...)Y_m \quad \text{.....(2.2)}$$

where A, B, C, etc. are undetermined coefficients that may be written in terms of the displacement parameters.

The displacement field for a simply supported finite strip is illustrated in Figure 2.3. The I is used to designate the Ith strip, and m represents the m^{th} harmonic. The deflection amplitudes w_{im} and w_{jm} at the two nodal lines i and j are chosen as the displacement parameters. The deflection functions at nodal lines i and j, respectively, are

$$\left.\begin{aligned} w_i &= \sum_{m=1}^{r} w_{im} Y_m \\ \text{and} \\ w_j &= \sum_{m=1}^{r} w_{jm} Y_m \end{aligned}\right\} \qquad \ldots\ldots\ldots\ldots\ldots\ldots\ldots\ldots\ldots\ldots\ldots\ldots\ldots\ldots\ldots\ldots\ldots\ldots (2.3)$$

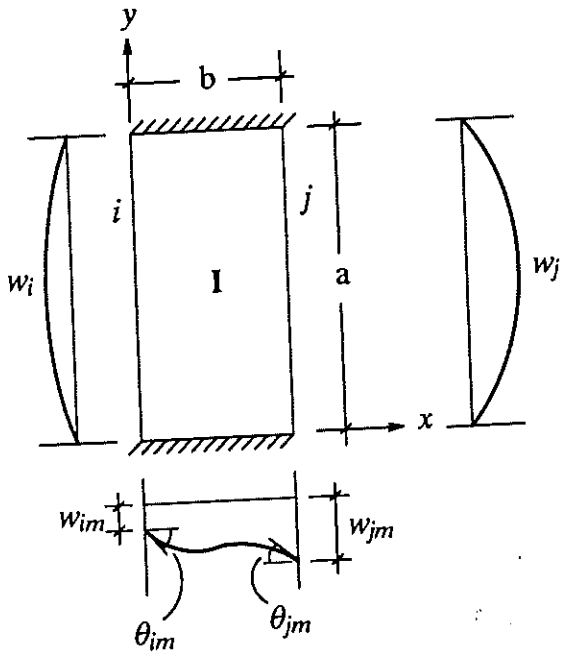

Figure 2.3. Displacement field for a simply supported finite strip.

The displacement field implies that, for two adjacent strips sharing a common nodal line i, the deflection amplitude w_{im} is the same for any harmonic m. However, this does not insure slope continuity across the strip boundaries and hence a smooth deflected surface does not exist for the entire continuum (*14*). In order to insure slope continuity, it is necessary to

specify two additional unknown parameters, namely the transverse slope amplitudes θ_{im} and θ_{jm} as shown in Figure 2.3. The transverse slope functions at nodal lines i and j, respectively, are

$$\left.\begin{aligned} \theta_i &= \left(\frac{\partial w}{\partial x}\right)_i = \sum_{m=1}^{r} \theta_{im} Y_m \\ \text{and} \\ \theta_j &= \left(\frac{\partial w}{\partial x}\right)_j = \sum_{m=1}^{r} \theta_{jm} Y_m \end{aligned}\right\} \quad \ldots\ldots\ldots\ldots\ldots\ldots\ldots\ldots\ldots\ldots\ldots\ldots\ldots\ldots (2.4)$$

As a stipulation of satisfying continuity of slope, it is necessary to employ only a third–order polynomial. The polynomial part of the displacement function now takes the form

$$f_m(x) = A + Bx + Cx^2 + Dx^3 \quad \ldots\ldots\ldots\ldots\ldots\ldots\ldots\ldots\ldots\ldots\ldots\ldots\ldots\ldots (2.5)$$

The constants A, B, C and D can now be written in terms of the four unknown displacement parameters w_{im}, θ_{im}, w_{jm} and θ_{jm}. This is accomplished by applying the following compatibility conditions

At $x=0$,

$$f_m(0) = w_{im}, \qquad \frac{\partial f_m(0)}{\partial x} = \theta_{im}$$

At $x=b$,

$$f_m(b) = w_{jm}, \qquad \frac{\partial f_m(b)}{\partial x} = \theta_{jm}$$

Using equation 2.5 and invoking the compatibility conditions, it follows that

$$\left.\begin{aligned} A &= w_{im} \\ B &= \theta_{im} \\ A + Bb + Cb^2 + Db^3 &= w_{jm} \\ B + 2Cb + 3Db^2 &= \theta_{jm} \end{aligned}\right\} \quad \ldots\ldots\ldots\ldots\ldots\ldots\ldots\ldots\ldots\ldots\ldots\ldots\ldots\ldots (2.6)$$

The solution of equation 2.6 for the constants A, B, C and D and substitution of the values into equation 2.2 results in a new form of the displacement function

$$w(x,y) = \sum_{m=1}^{r} \left\{ \left(1 - \frac{3x^2}{b^2} + \frac{2x^3}{b^3} \right) w_{im} + \left(x - \frac{2x^2}{b} + \frac{x^3}{b^2} \right) \theta_{im} + \left(\frac{3x^2}{b^2} - \frac{2x^3}{b^3} \right) w_{jm} + \left(\frac{x^3}{b^2} - \frac{x^2}{b} \right) \theta_{jm} \right\} Y_m \quad \ldots\ldots\ldots\ldots\ldots\ldots\ldots\ldots (2.7)$$

In matrix form, equation 2.7 can be written as:

$$w(x,y) = \sum_{m=1}^{r} [N_1, N_2, N_3, N_4] \begin{bmatrix} w_{im} \\ \theta_{im} \\ w_{jm} \\ \theta_{jm} \end{bmatrix} Y_m \quad \ldots\ldots\ldots\ldots\ldots\ldots\ldots\ldots\ldots\ldots\ldots\ldots\ldots\ldots (2.8)$$

or more simply,

$$w_I(x,y) = \sum_{m=1}^{r} [N]_I \{\delta_m\}_I Y_m \quad \ldots\ldots\ldots\ldots\ldots\ldots\ldots\ldots\ldots\ldots\ldots\ldots\ldots\ldots\ldots\ldots (2.9)$$

where $[N]_I$ is a matrix containing shape functions for I^{th} strip and $\{\delta_m\}_I$ contains the various displacements for I^{th} strip.

A shape function is a polynomial that defines the displacement field resulting from a nodal displacement. For the simply supported strip shown in Figure 2.3, there are four displacement parameters w_{im}, θ_{im}, w_{jm} and θ_{jm}. The shape function for each one of these

degrees of freedom (DOF) is derived by allowing an individual DOF to displace a unit amount while restraining all other DOF at zero. The shape functions associated with the four DOF are shown in Figure 2.4.

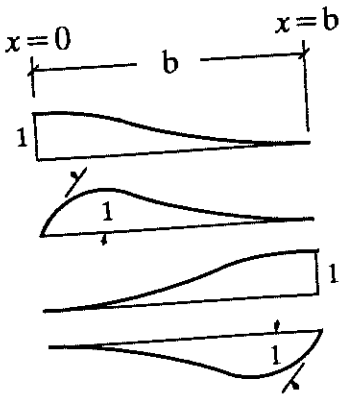

	At $x=0$		At $x=b$	
	N_i	$N_{i,x}$	N_i	$N_{i,x}$
$N_1 = 1 - \frac{3x^2}{b^2} + \frac{2x^3}{b^3}$	1	0	0	0
$N_2 = x - \frac{2x^2}{b} + \frac{x^3}{b^2}$	0	1	0	0
$N_3 = \frac{3x^2}{b^2} - \frac{2x^3}{b^3}$	0	0	1	0
$N_4 = \frac{x^3}{b^2} - \frac{x^2}{b}$	0	0	0	1

Figure 2.4. Shape functions of a third–order polynomial fitted to ordinates and slopes at $x=0$ and at $x=b$.

2.2.2. SERIES PART OF DISPLACEMENT FUNCTION

The second part of the displacement function (equation 2.1) is the series part (Y_m). One of the most commonly used series is the eigenfunctions derived from the solution of the spatial portion of the beam vibration differential equation (*8*).

$$Y'''' = \frac{\mu^4}{a^4} Y \qquad \ldots\ldots\ldots\ldots\ldots\ldots\ldots\ldots\ldots\ldots\ldots\ldots\ldots\ldots\ldots\ldots\ldots\ldots\ldots\ldots (2.10)$$

where a is the length of the beam, in this case the length of a strip, and μ is a general parameter.

The solution to the differential equation shown in equation (2.10) is

$$Y(y) = C_1 \sin\left(\frac{\mu y}{a}\right) + C_2 \cos\left(\frac{\mu y}{a}\right) + C_3 \sinh\left(\frac{\mu y}{a}\right) + C_4 \cosh\left(\frac{\mu y}{a}\right) \qquad \ldots\ldots\ldots (2.11)$$

The unknown coefficients C_1, C_2, C_3 and C_4 are determined by applying appropriate

boundary conditions. For the case where the strips are simply supported, the boundary conditions require that both the displacement ($Y(y)$) and the bending moment ($Y''(y)$) equal zero at the two ends of the strip. Invoking the following boundary conditions ($Y(0)=Y''(0)=0$, $Y(a)=Y''(a)=0$), the form of the series function becomes

$$Y_m(y) = \sin\left(\frac{m\pi y}{a}\right) \quad (m = 1,2,3,\ldots) \qquad \ldots\ldots\ldots\ldots\ldots\ldots\ldots\ldots\ldots (2.12)$$

For the case where the strips are assumed to be simply supported on one end and fixed on the other end, the boundary conditions require that ($Y(0)=Y''(0)=0$, $Y(a)=Y'(a)=0$). The form of the series function becomes

$$\left.\begin{aligned} Y_m(y) &= \sin\left(\frac{\mu_m y}{a}\right) - a_m \sinh\left(\frac{\mu_m y}{a}\right) \\ a_m &= \frac{\sin\mu_m}{\sinh\mu_m} \\ \mu_m &= \frac{4m+1}{4}\pi \end{aligned}\right\} \qquad \ldots\ldots\ldots\ldots\ldots\ldots\ldots\ldots\ldots (2.13)$$

For the case where the strips are assumed to have both ends fixed, the boundary conditions require that ($Y(0)=Y'(0)=0$, $Y(a)=Y'(a)=0$). The form of the series function becomes

$$\left.\begin{aligned} Y_m(y) &= \sin\left(\frac{\mu_m y}{a}\right) - a_m \sinh\left(\frac{\mu_m y}{a}\right) - a_m\left[\cos\left(\frac{\mu_m y}{a}\right) - \cosh\left(\frac{\mu_m y}{a}\right)\right] \\ a_m &= \frac{\sin\mu_m - \sinh\mu_m}{\cos\mu_m - \cosh\mu_m} \\ \mu_m &= \frac{2m+1}{2}\pi \end{aligned}\right\} \qquad \ldots\ldots\ldots (2.14)$$

The primary reason for using the basic functions as the series representation is the fact that they are orthogonal, or stated mathematically

$$\left.\begin{aligned} &\int_0^a Y_m Y_n \, dy = 0 \\ &\int_0^a Y'_m Y'_n \, dy = 0 \end{aligned}\right\} \text{ for } m \neq n \quad \ldots\ldots\ldots\ldots\ldots\ldots\ldots\ldots\ldots\ldots \quad (2.15)$$

These relationships are of great importance, particularly in the finite strip method. For a model containing n nodes in which m terms are to be considered in the summation, the m sets of n nodal parameters for each term can be solved separately and then superimposed (25). If orthogonality is not present, the simultaneous solution of m x n sets of parameters would be required. Orthogonality has even more importance in the formulation of the strip stiffness matrix. As will be observed, the integrals in equation (2.15) appear several times in subsequent formulations. The orthogonality relationships dramatically simplify the strip stiffness matrices, and using these relationships reduces the computational effort significantly.

For the purpose of this investigation, only simply supported flat plate systems are considered. With the inclusion of different boundary conditions, equations (2.13) and (2.14), the set of strip stiffness equations do not uncouple as they do when using equation (2.12).

2.3. MATRIX FORMULATION

All of the equations and matrix formulations to this point have been devoted to relating the nodal displacement parameters to the displacement function of the individual strip. The following sections concentrate on the relationships between the displacement functions and the generalized strains, the relationship between stresses and strains, and

formulation of the strain energy of the finite strips. The individual strip equations are assembled into an overall set of system equations that define the behavior of the entire continuum.

2.3.1. DISPLACEMENT FUNCTIONS

Recall the form of the displacement function for an individual strip, equation (2.1)

$$f = w(x,y) = \sum_{m=1}^{r} f_m(x)Y_m$$

The general form of the displacement functions can be defined as

$$\{f\} = \sum_{m=1}^{r} [[N_1][N_2]\ldots]\begin{Bmatrix}\{\delta_1\}\\ \{\delta_2\}\\ \vdots\end{Bmatrix}_m Y_m$$

$$= \sum_{m=1}^{r} Y_m \sum_{k=1}^{s} [C_k]\{\delta_k\}_m \qquad \text{(2.16a)}$$

The $m=1, 2, \ldots, r$ refers to the number of harmonics included in the series, and $k=1, 2, \ldots, s$ refers to the number of nodal lines used to discretize the continuum.

The expressions in equation (2.16a) can be simplified by combining both the series and the shape functions in the following way

$$\{f\} = \sum_{m=1}^{r} \sum_{k=1}^{s} [N_k]_m\{\delta_k\}_m$$

$$= \sum_{m=1}^{r} [N]_m\{\delta\}_m$$

$$= [N]\{\delta\} \qquad \text{(2.16b)}$$

2.3.2. STRAINS

Once the displacement functions are known, the generalized strains are obtained through differentiation with respect to the coordinates x and y. These "...generalized strains include normal and shear strain as well as bending and twisting curvatures." (*8*). The generalized strains are

$$\{\epsilon\} = [B]\{\delta\}$$

$$= \sum_{m=1}^{r} [B]_m\{\delta\}_m$$

$$= \sum_{m=1}^{r} \sum_{k=1}^{s} [B_k]_m\{\delta_k\}_m \qquad (2.17)$$

For a bending strip, the strains are

$$\{\epsilon\} = \begin{Bmatrix} \chi_x \\ \chi_y \\ \chi_{xy} \end{Bmatrix} = \begin{Bmatrix} \dfrac{-\partial^2 w}{\partial x^2} \\ \dfrac{-\partial^2 w}{\partial y^2} \\ 2\dfrac{\partial^2 w}{\partial x \partial y} \end{Bmatrix} \qquad (2.18a)$$

The strain matrix then becomes

$$[B] = \begin{bmatrix} \dfrac{-\partial^2[N]}{\partial x^2} \\ \dfrac{-\partial^2[N]}{\partial y^2} \\ 2\dfrac{\partial^2[N]}{\partial x \partial y} \end{bmatrix} \qquad (2.18b)$$

2.3.3. STRESSES

The stresses (bending moments) are related to the strains by a property matrix containing material properties of the strip

$$\{\sigma\} = \begin{Bmatrix} M_x \\ M_y \\ M_{xy} \end{Bmatrix} = [D]\{\epsilon\} = [D][B]\{\delta\}$$

$$= [D] \sum_{m=1}^{r} [B]_m \{\delta\}_m$$

$$= [D] \sum_{m=1}^{r} \sum_{k=1}^{s} [B_k]_m \{\delta_k\}_m \qquad \ldots\ldots\ldots\ldots\ldots\ldots\ldots\ldots\ldots\ldots\ldots\ldots\ldots\ldots (2.19)$$

The property matrix $[D]$ used here is referred to as the elasticity matrix. For an orthotropic plate in bending, the elasticity matrix is

$$[D] = \begin{bmatrix} D_x & D_1 & 0 \\ D_1 & D_y & 0 \\ 0 & 0 & D_{xy} \end{bmatrix} \qquad \ldots\ldots\ldots\ldots\ldots\ldots\ldots\ldots\ldots\ldots\ldots\ldots\ldots\ldots\ldots\ldots\ldots\ldots (2.20)$$

The individual elements of the elasticity matrix (D_x, D_y, D_1 and D_{xy}) are defined as the orthotropic plate constants given by

$$D_x = \frac{E_x t^3}{12(1 - \nu_x \nu_y)}$$

$$D_y = \frac{E_y t^3}{12(1 - \nu_x \nu_y)}$$

$$D_1 = \frac{\nu_x E_y t^3}{12(1 - \nu_x \nu_y)} = \frac{\nu_y E_x t^3}{12(1 - \nu_x \nu_y)}$$

$$D_{xy} = \frac{Gt^3}{12}$$

where:

E_x = Modulus of elasticity in the x direction
E_y = Modulus of elasticity in the y direction
ν_x = Poisson's ratio in the x direction
ν_y = Poisson's ratio in the y direction
t = Plate strip thickness
G = Shear modulus

2.3.4. MINIMIZATION OF TOTAL POTENTIAL ENERGY

(a) Strain energy

The strain energy of an elastic body is defined as

$$U = \frac{1}{2}\int_V \{\epsilon\}^T\{\sigma\}\, dV \qquad \text{(2.21a)}$$

Using the equations developed for strains (2.17) and stresses (2,19), equations, equation (2.21a) can be rewritten as

$$U = \frac{1}{2}\int_V \{\delta\}^T[B]^T[D][B]\{\delta\}\, dV \qquad \text{(2.21b)}$$

(b) Potential energy

The potential energy due to the external loads $\{q\}$ acting on the individual strips is given by

$$W = -\int_A \{f\}^T\{q\}\, dA \qquad \text{(2.22a)}$$

and substitution of equation (2.16b) into (2.22a) gives

$$W = -\int_A \{\delta\}^T [N]^T \{q\}\, dA \qquad \ldots\ldots (2.22b)$$

(c) Total potential energy

The total potential energy (ϕ) of an elastic body is defined as the sum of the internal stain energy (U) stored in the body and the potential energy of the loads (W).

$$\phi = U + W$$

$$= \frac{1}{2}\int_V \{\delta\}^T [B]^T [D][B]\{\delta\}\, dV - \int_A \{\delta\}^T [N]^T \{q\}\, dA \qquad \ldots\ldots (2.23)$$

(d) Minimization procedure

The principle of minimum total potential energy, also known as stationary potential energy, is used quite often in structural mechanics. The principle states that

> *Among all admissible configurations of a conservative system, those that satisfy the equations of equilibrium make the potential energy stationary with respect to small admissible variations of displacement.* (9).

Mathematically the principle of stationary potential energy requires that

$$\left\{\frac{\partial \phi}{\partial \{\delta\}}\right\} = \{0\} \qquad \ldots\ldots (2.24)$$

Substitution of the expression for total potential energy, equation (2.23), into equation (2.24) and performing the required partial differentiation gives

$$\left\{\frac{\partial \phi}{\partial \{\delta\}}\right\} = \int_V [B]^T [D][B]\{\delta\}\, dV - \int_A [N]^T \{q\}\, dA = \{0\} \qquad \ldots\ldots (2.25)$$

(e) Stiffness matrix

In matrix notation equation (2.25) can be rewritten as

$$[S]\{\delta\} - \{F\} = \{0\} \quad \ldots\ldots (2.26)$$

where $[S]$ is the stiffness matrix, $\{\delta\}$ is the nodal displacement vector and $\{F\}$ is the load vector. The stiffness matrix takes the form

$$[S] = \int_V [B]^T [D][B]\{\delta\}\, dV$$

which can be rewritten as

$$[S] = \begin{bmatrix} [S]_{11}\,[S]_{12} \ldots [S]_{1r} \\ [S]_{21}\,[S]_{22} \ldots [S]_{2r} \\ \ldots \quad \ldots \quad \ldots \quad \ldots \\ [S]_{r1}\,[S]_{r2} \ldots [S]_{rr} \end{bmatrix} \quad \ldots\ldots (2.27a)$$

with

$$[S]_{mn} = \int_V [B]_m^T [D][B]_n\{\delta\}\, dV \quad \ldots\ldots (2.27b)$$

because of the property of orthogonality, equation (2.27a) takes the form

$$[S] = \begin{bmatrix} [S]_{11} & 0 & \ldots & 0 \\ 0 & [S]_{22} & \ldots & 0 \\ \ldots & \ldots & \ldots & \ldots \\ 0 & 0 & \ldots & [S]_{rr} \end{bmatrix} \quad \ldots\ldots (2.27c)$$

By comparing equations (2.27a) and (2.27c) the value of the orthogonality relationships can be readily seen. As a result of the orthogonality relationships, the individual model stiffness

matrices are grouped on the matrix diagonal, which in turn results in a significantly reduces computational effort. It should be noted that this decoupling effect is a result of the simply supported boundary condition and does not occur in general.

(f) Consistent load matrix

From equation (2.25) the load matrix is interpreted as

$$\{F\} = \int_A [N]^T \{q\}\, dA \qquad \ldots\ldots (2.28)$$

for the mth term in the series, the load matrix becomes

$$\{F\}_m = \int_A [N]_m^T \{q\}\, dA \qquad \ldots\ldots (2.29)$$

For a uniformly distributed load over the entire area of the strip

$$\{F\}_m = q \int_0^b [N]_m^T dx \int_0^a Y_m dy$$

$$= q \begin{Bmatrix} \frac{b}{2} \\ \frac{b^2}{12} \\ \frac{b}{2} \\ \frac{-b^2}{12} \end{Bmatrix} \int_0^a Y_m dy \qquad \ldots\ldots (2.30)$$

For a uniform patch load of magnitude Q_o located on the strip at coordinates (x_1, y_1) and (x_2, y_2), equation (2.29) becomes

$$\{F\}_m = Q_o \begin{Bmatrix} \bar{x} - \dfrac{\bar{x}^3}{b^2} + \dfrac{\bar{x}^4}{2b^3} \\ \dfrac{\bar{x}^2}{2} - \dfrac{2\bar{x}^3}{3b} + \dfrac{\bar{x}^4}{4b^2} \\ \dfrac{\bar{x}^3}{b^2} - \dfrac{\bar{x}^4}{2b^3} \\ \dfrac{\bar{x}^4}{4b^2} - \dfrac{\bar{x}^3}{3b} \end{Bmatrix} \int_0^a Y_m dy$$

where $\bar{x}^n = x_2^n - x_1^n$ ..... (2.31)

For a concentrated load P_c located on the strip at coordinates $x=x_c$, $y=y_c$, equation (2.29) is simplified by the fact that the coordinates of the load can be substituted directly into the equation without the need for evaluating the integral. Therefore for a concentrated load, the load matrix becomes

$$\{F\}_m = P_c y_c Y_m \begin{Bmatrix} (1 - 3\bar{x}_c^2 + 2\bar{x}_c^3) \\ x_c(1 - 2\bar{x}_c + \bar{x}_c^2) \\ (3\bar{x}_c^2 - 2\bar{x}_c^3) \\ x_c(\bar{x}_c^2 - \bar{x}_c) \end{Bmatrix}$$

where $\bar{x}_c = \dfrac{x_c}{b}$ ..... (2.32)

2.4. STIFFNESS CONTRIBUTION OF AN ELASTIC BEAM

For the purpose of this investigation it was necessary to incorporate both the axial and the flexural stiffnesses of elastic beams to the stiffness of the individual strips to which they are attached. The stiffness of an individual bending strip has already been established in the previous sections, and it will be shown that both the axial and flexural stiffness of an elastic beam can be directly added to the strip stiffness matrix.

An example of an individual bending strip supported by an elastic beam is shown below in Figure 2.5.

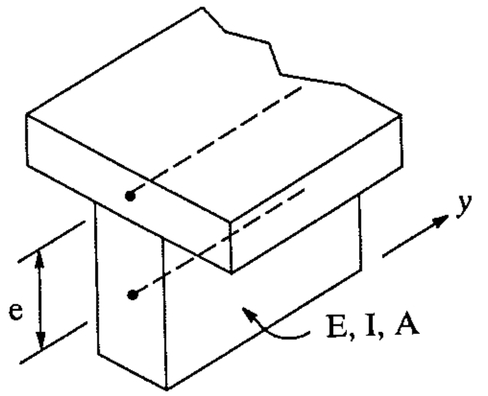

Figure 2.5. Typical finite strip supported by an elastic beam.

Recall the form of the displacement function for an individual finite strip in bending is

$$w = \sum_{m=1}^{\infty}\left(\sin\frac{m\pi y}{l}\right)\delta_m \qquad (2.33)$$

The flexural strain energy of the beam is defined as

$$U = \frac{1}{2}EI\int_0^L\left(\frac{\partial^2 w}{\partial y^2}\right)^2 dy \qquad (2.34)$$

The stiffness of the beam can be derived by using the following relationship

$$k_m = \frac{\partial^2 U}{\partial\delta_m^2} = EI\int_0^L\left(\frac{\partial^2 w}{\partial y^2}\right)\frac{\partial}{\partial\delta_m}\left(\frac{\partial^2 w}{\partial y^2}\right)dy \qquad (2.35a)$$

Combining equations (2.33) and (2.34) into (2.35a), the stiffness of the beam becomes

$$= EI\int_0^L\frac{\partial}{\partial y^2}\left(\sum_{m=1}^{\infty}\sin\frac{m\pi y}{l}\right)\delta_m\frac{\partial}{\partial\delta_m}\left(\frac{\partial}{\partial y}\sum_{n=1}^{\infty}\sin\frac{n\pi y}{l}\right)\delta_m dy \qquad (2.35b)$$

By performing the partial differentiation, and noticing that

$$\frac{\partial}{\partial \delta_m}\left(\frac{\partial}{\partial y}\sum_{n=1}^{\infty}\sin\frac{n\pi y}{l}\right)\delta_m = \sum_{n=1}^{\infty}\sin\frac{n\pi y}{l}$$

the beam stiffness equation can be reduced to

$$EI\int_0^L\left(-\frac{m^2\pi^2}{l^2}\sum_{m=1}^{\infty}\sin\frac{m\pi y}{l}\delta_m\right)\left(-\frac{n^2\pi^2}{l^2}\sum_{n=1}^{\infty}\sin\frac{n\pi y}{l}\right)dy \qquad \ldots\ldots\ldots\ldots (2.35c)$$

which can be written in an expanded series format

$$EI\frac{m^2n^2\pi^4}{l^4}\int_0^L\left[\sin\frac{\pi y}{l}\delta_1 + \sin\frac{2\pi y}{l}\delta_2 + \sin\frac{3\pi y}{l}\delta_3 + \cdots\right]$$
$$\left[\sin\frac{\pi y}{l} + \sin\frac{2\pi y}{l} + \sin\frac{3\pi y}{l} + \cdots\right]dy \qquad \ldots\ldots\ldots\ldots\ldots\ldots (2.35d)$$

Recall the orthogonality property of sine functions

$$\int_0^L \sin\frac{m\pi y}{l}\sin\frac{n\pi y}{l}\begin{cases} 0 \text{ for } m \neq n \\ \frac{L}{2} \text{ for } m = n \end{cases}$$

Using this relationship while performing the integration, the stiffness of the beam reduces to

$$k_m = EI\left(\frac{m^4\pi^4}{L^4}\right)\left(\frac{L}{2}\right)$$
$$= EI\frac{m^4\pi^4}{2L^3} \qquad \ldots\ldots\ldots\ldots\ldots\ldots\ldots\ldots\ldots\ldots\ldots\ldots\ldots\ldots (2.35e)$$

The axial strain energy of the beam is defined as

$$U = \frac{1}{2}\int_0^L EA\left(\frac{\partial u}{\partial y}\right)^2 dy \qquad \text{(2.36a)}$$

where u is the axial displacement. Equation (2.36a) reduces to

$$= \frac{1}{2}EAe^2\int_0^L \left(\frac{\partial^2 w}{\partial y^2}\right)^2 dy \qquad \text{(2.36b)}$$

Comparing the similarities between equation (2.34) and (2.36b), it should be noted that the same process can be used to derive at the added stiffness due to the beam eccentricity

$$k_m = EAe^2\frac{m^4\pi^4}{2L^3} \qquad \text{(2.37)}$$

The two stiffnesses, equations (2.35e) and (2.37), can be combined to form the total flexural stiffness.

$$k_m = \left(EI + EAe^2\right)\frac{m^4\pi^4}{2L^3} \qquad \text{(2.38a)}$$

Notice that the terms within the parenthesis can be combined to form an equivalent flexural stiffness, EI_{EQ}.

$$k_m = EI_{EQ}\frac{m^4\pi^4}{2L^3} \qquad \text{(2.38b)}$$

Through direct superposition, the flexural stiffness for an elastic beam is added to the stiffness matrix of the finite strip to which the beam is attached.

2.5. APPLICATION OF THE FINITE STRIP METHOD

The finite strip method lends itself to plate continua with regular geometry and continuous boundary conditions. Due to the fact the geometry of a bridge deck is fairly regular and the boundary conditions do not vary along the width, the FSM is very well suited for the analysis of bridge decks.

The numerical operations given in this chapter were incorporated in a computer program based on the compound strip algorithm described by Puckett (*18*). In 1986 Wiseman (*25*) expanded the program to include the analysis capability for folded plate structures. This revised program was designed primarily to test algorithms and equations and lacked many of the features common in production software.

For the purpose of this investigation, a problem oriented language system (POL) was used for an enhanced user interface. The program was adapted primarily to be used by bridge engineers. Several of the procedures for the FSM were automated such as nodal definition and mesh generation. This makes it possible for a bridge to be defined in engineering terms such as span, deck thickness, girder spacing, etc.

An algorithm for the revised program is presented in Appendix A. It is the author's intent that this revised program will be incorporated into BRASS (Bridge Rating and Analysis of Structural Systems) version 5. "BRASS is a system of computer programs developed to assist the bridge engineer in the designing and determining the load capacity of highway bridges." (*6*) The revised program was named BRASS-DISTRIBUTION FACTOR (BRASS-DIST for short) and the software documentation is presented in Appendix B.

CHAPTER 3

VERIFICATION PROBLEMS

To ensure that the finite strip method program was accurately representing the behavior of a thin plate, it was necessary perform a series of verification problems. These particular problems were chosen to test various boundary conditions and load types. These problems were also used to test the sensitivity of the solution to both the number of terms, or harmonics, included in the summation and the number of strips used to discretize the domain. The various solutions obtained by the computer program were compared with closed–form solutions developed by Timoshenko in *Theory of Plates and Shells* (*24*).

3.1. RECTANGULAR PLATE SIMPLY SUPPORTED ON TWO EDGES

The first verification problem is a uniformly loaded rectangular plate, simply supported on two edges with the other two edges free as shown in Figure 3.1.

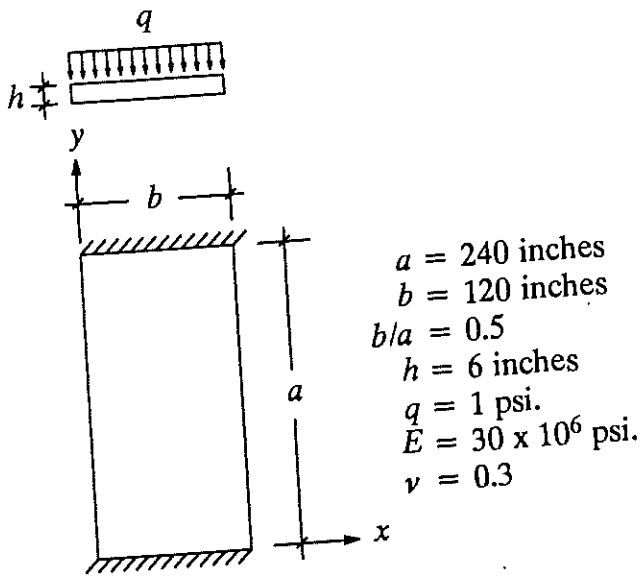

Figure 3.1. Rectangular plate simply supported on two edges.

The flexural rigidity (D) of the plate is defined as

$$D = \frac{Eh^3}{12(1-\nu^2)}$$

$$= \frac{30 \times 10^6 \text{psi.}(6\text{in.})^3}{12\left(1-(0.3)^2\right)}$$

$$= 593{,}406{,}593 \text{ lb·in}$$

The maximum deflection (Δ_{max}) for this problem occurs at the plate center ($x=b/2, y=a/2$) and is defined as

$$\Delta_{max} = \alpha\frac{qa^4}{D}$$

$$= 0.01377\frac{1\text{psi.}(240\text{in.})^4}{593,406,593 \text{ lb}\cdot\text{in}}$$

$$= 0.07698 \text{ in.}$$

where α is a numerical factor depending on the ratio b/a of the sides of the plate given by Timoshenko (*24*).

The maximum bending moments, taken about both axes x and y, also occur at the plate center and are defined as

$$(M_x)_{max} = \beta_1 q a^2$$
$$= 0.1235(1\text{psi.})(240\text{in.})^2$$
$$= 7113 \text{ lb·in}$$

$$(M_y)_{max} = \beta_1' q a^2$$
$$= 0.0122(1\text{psi.})(240\text{in.})^2$$
$$= 702.7 \text{ lb·in}$$

The numerical values of the factors β_1 and β_1' (see footnote) are also given by Timoshenko (*24*).

The verification problem was then analyzed using the computer program. The number of strips used to discretize the plate was first set at ten, and then allowed to increase. Both maximum deflection (Δ_{max}) and maximum bending moments $(M_x)_{max}$ and $(M_y)_{max}$ were determined at the middle surface of the plate. In the analysis the number of terms included in the summation started at one and was increased until convergence was reached.

The numerical value for β_1' given above was not verified with Timoshenko, however values of β_1' for all other aspect ratios were confirmed, and it was determined that an error exists in the referenced value of β_1' for this particular aspect ratio.

Convergence is the property exhibited when a solution parameter, in this case deflection and bending moment, ceases to change as the finite strip model is refined. Although convergence is necessary, it in itself is not sufficient to fully verify solution accuracy. It is very possible to converge to the wrong solution. Therefore, in addition to convergence, it is also necessary to converge to the correct or "exact" solution.

The first solution parameter that was verified was maximum deflection. This is shown graphically in Figure 3.2. It is instructive to note that with only including the first harmonic, the deflection obtained by the FSM has less than one half of one percent error as compared to *Theory of Plates and Shells* (*24*). It is also important to note the rate of convergence for maximum deflection is very fast. Within the first four terms, the maximum deflection has converged to the correct solution (within 0.04% error).

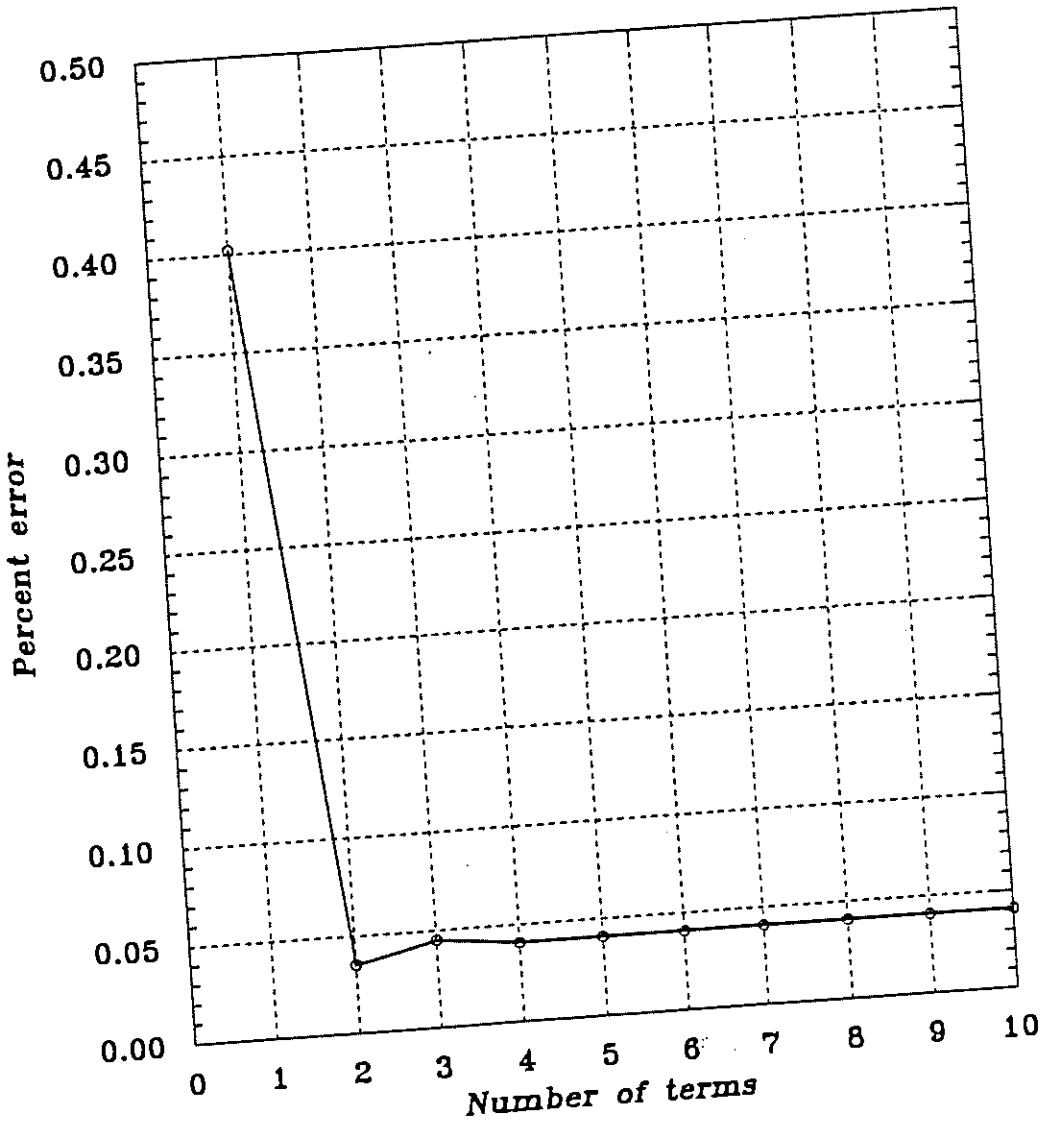

Figure 3.2. Convergence of maximum deflection (Δ_{max}) in a rectangular plate with two edges simply supported and two edges free.

The next solution parameter that was verified was the maximum bending moments in the plate. The bending moment (M_x) is defined as the bending moment that causes a flexural bending stress in the y–direction, and conversely, (M_y) causes a flexural bending stress in the x–direction. The convergence of maximum bending moments is demonstrated in Figure 3.3. It is readily observed that the solution convergence is not monotonic, but rather oscillatory in nature. Monotonic convergence would result if by increasing the number of terms, the percent error consistently decreased until some final value. Note that the even terms do not contribute in this problem due to the symmetry of both structure and load about $y = 120$ inches.

Comparing both $(M_x)_{max}$ and $(M_y)_{max}$ in Figure 3.3, the convergence rates are approximately the same, but the convergence toward the correct solution is different. Recall that the displacement functions used in the FSM are a combination of hermitian polynomials in the transverse (x) direction and continuously differentiable smooth series in the longitudinal (y) direction. The assumed displacement functions used for simply supported strips are

$$w(x,y) = \sum_{m=1}^{r} f_m(x) Y_m(y)$$
$$= \sum_{m=1}^{r} \left(A + Bx + Cx^2 + Dx^3\right) \sin\left(\frac{m\pi y}{a}\right) \quad \ldots\ldots\ldots\ldots\ldots\ldots\ldots\ldots (3.1)$$

where A, B, C and D are arbitrary constants defined in the previous chapter.

The expressions for determining both bending moments are given as

$$\left.\begin{aligned} M_x &= D\left(\frac{\partial^2 w}{\partial x^2} + \nu\frac{\partial^2 w}{\partial y^2}\right) \\ M_y &= D\left(\frac{\partial^2 w}{\partial y^2} + \nu\frac{\partial^2 w}{\partial x^2}\right) \end{aligned}\right\} \qquad (3.2)$$

where D is the flexural rigidity of the plate defined earlier. Notice that in equation (3.2), M_x is determined predominantly by the first term, the second partial of the displacement function with respect to x. Likewise, M_y is determined predominantly by the second partial of the displacement function with respect to y.

The series function in the y-direction is a better approximating function than the polynomial function in the x-direction. For this reason M_y, the bending moment that causes a flexural bending stress in the x-direction, has a greater error associated with it than M_x, and this is evident in Figure 3.3.

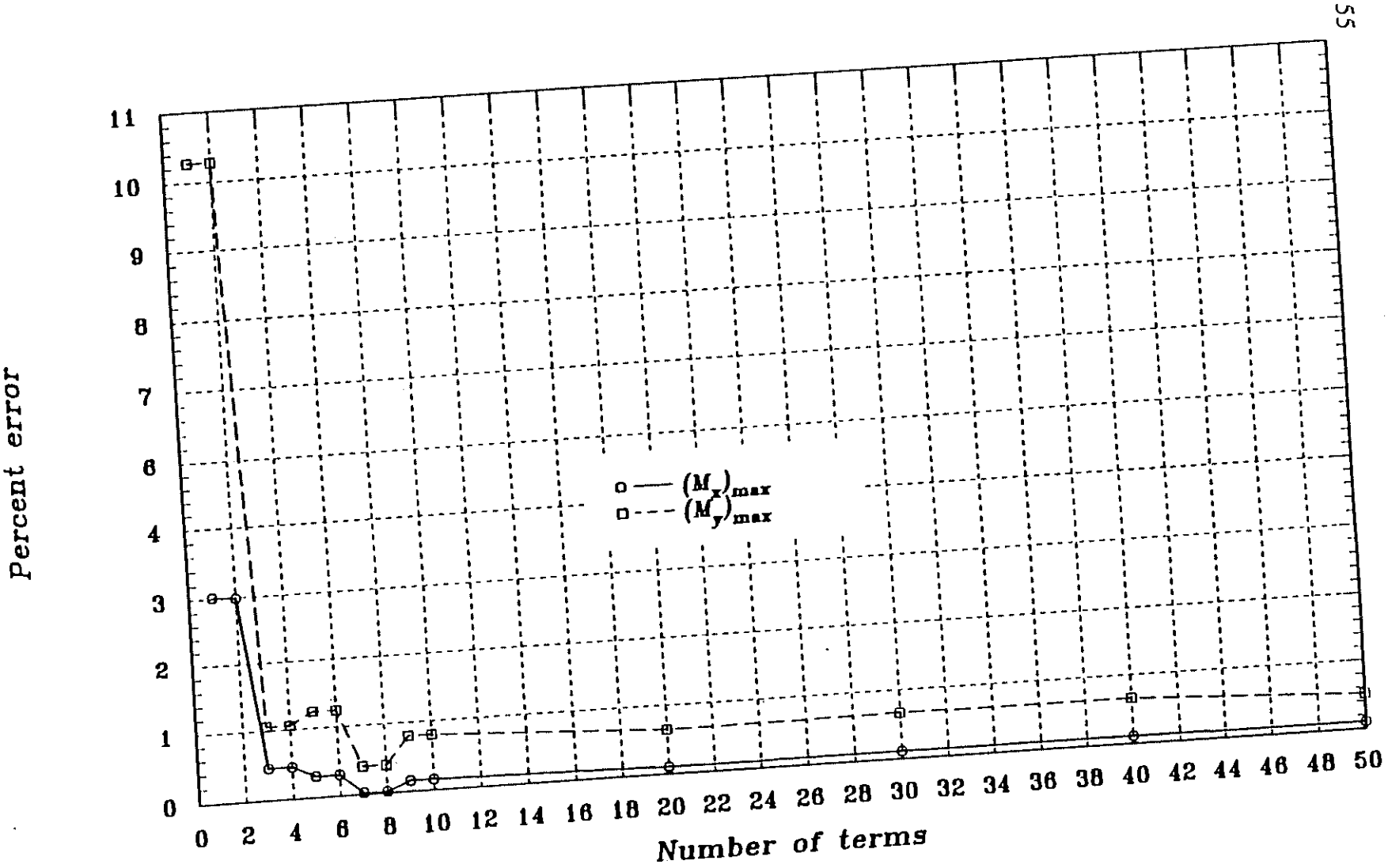

Figure 3.3. Convergence of maximum bending moments $(M_x)_{max}$ and $(M_y)_{max}$ in a rectangular plate with two edges simply supported and two edges free.

While the solution is sensitive to the number of terms, it is also sensitive to the number of strips used to discretize the plate. A comparison between $(M_x)_{max}$ as determined from two different analyses is presented in Figure 3.4. In the first analysis the number of strips used was set at ten, and in the second analysis the number of strips was increased to fifty. Notice that in Figure 3.4 the two curves lie on top of one another, which implies that ten strips is sufficient for the determination of $(M_x)_{max}$.

A similar comparison was made for $(M_y)_{max}$, the results of which are presented in Figure 3.5. It is important to notice that the solution for $(M_y)_{max}$ is sensitive to the number of strips used to discretize the plate. This is also a result of M_y being determined by the second partial of the displacement function with respect to y (equation 3.2). To insure convergence had been reached with the number of strips, a third analysis was performed with one hundred strips through the plate. Notice that in Figure 3.5 there is no significant increase in solution accuracy in increasing the number of strips from fifty to one hundred.

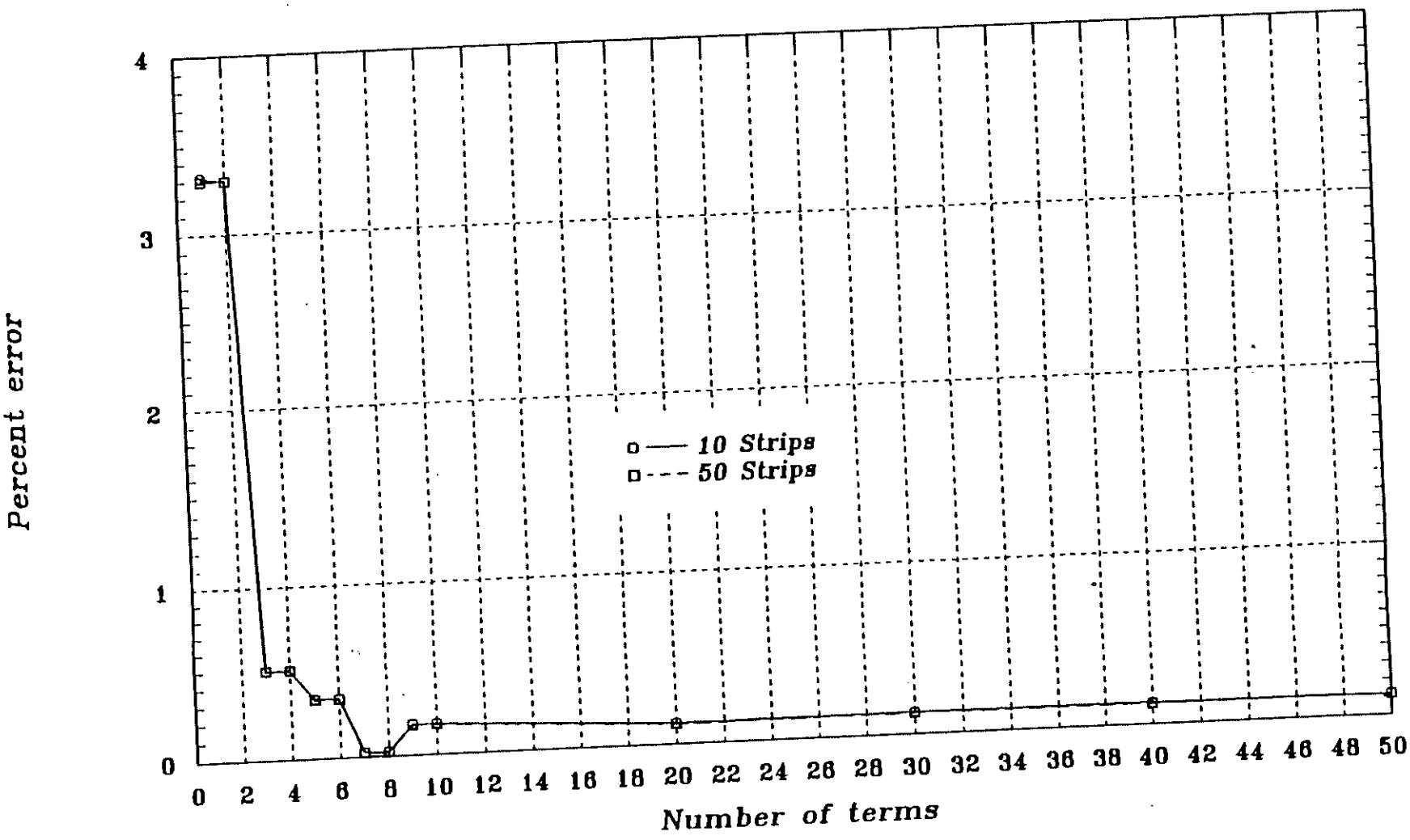

Figure 3.4. Comparison of maximum bending moment $(M_x)_{max}$ for different numbers of strips used to discretize the plate.

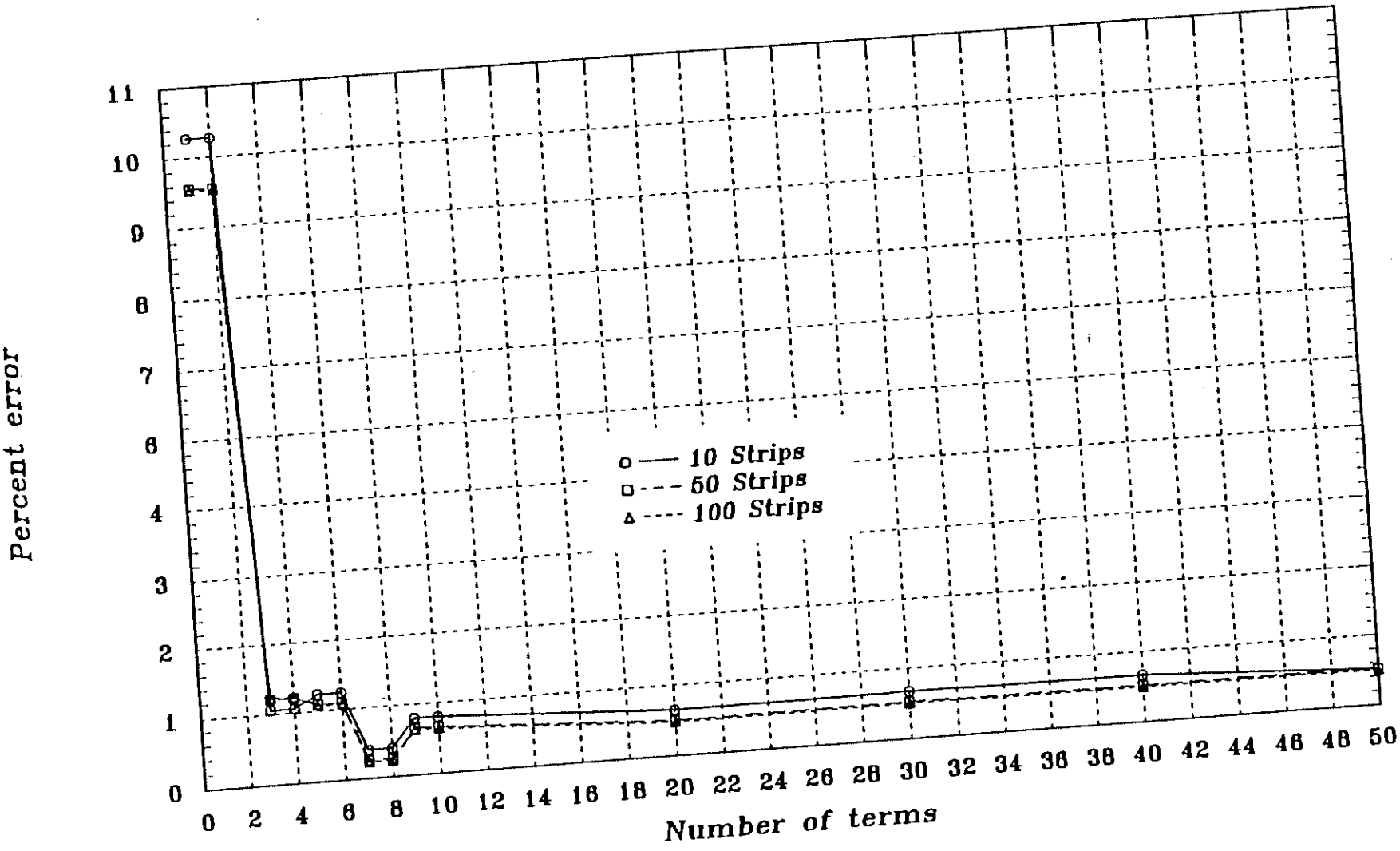

Figure 3.5. Comparison of maximum bending moment $(M_y)_{max}$ for different numbers of strips used to discretize the plate.

3.2. SQUARE PLATE SIMPLY SUPPORTED ON TWO EDGES WITH THE OTHER TWO EDGES SUPPORTED BY ELASTIC BEAMS

The second verification problem is shown in Figure 3.6. This problem was used to test the composite action of the plate with the elastic beams, a situation more closely resembling a bridge deck supported by girders.

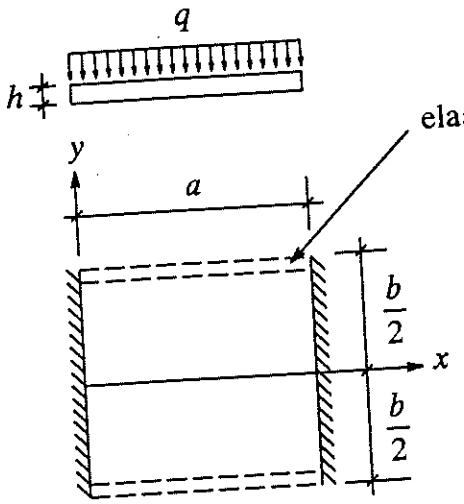

a = 120 inches
b = 120 inches
b/a = 1
h = 6 inches
q = 1 psi.
E = 30 x 10^6 psi.
ν = 0.3

Figure 3.6. Square plate simply supported on two edges with the other two edges supported by elastic beams.

To test the relationship between the plate and the supporting beams, the flexural rigidity of the elastic beams (EI) was varied from zero to infinity. In order to relate the flexural rigidity of the supporting beams (EI) to the flexural rigidity of the plate (D), it was necessary to define a parameter (λ) given as

$$\lambda = \frac{EI}{aD}$$

Fortunately, the solution to this problem has been previously established and can be found in *Theory of Plates and Shells* (*24*). Maximum deflections and bending moments for several different values of λ have been determined and are summarized in Table 3.1.

Table 3.1. Maximum plate actions as a function of beam flexural rigidity.

λ parameter	*Flexural rigidity*	*Deflection*	*Bending moments*	
$\lambda = \frac{EI}{aD}$	EI	Δ_{max}	$(M_x)_{max}$	$(M_y)_{max}$
∞	∞	0.0014	689.7	689.7
100	7.121E+12	0.0014	692.6	686.8
10	7.121E+11	0.0015	720.0	669.6
1	7.121E+10	0.0021	925.9	541.4
0	0	0.0045	1764	390.2

This problem was then analyzed using the computer program with several different values of λ. The first solution parameter that was verified was maximum deflection. The convergence for the maximum deflection in the plate is shown in Figure 3.7. With the addition of supported beams to the plate, the first nine harmonics are required for convergence, compared to four harmonics in the first verification problem.

The convergence of maximum bending moments in the plate $(M_x)_{max}$ and $(M_y)_{max}$ is presented in Figures 3.8 and 3.9, respectively. If the supporting beams are absolutely rigid, $\lambda = \infty$, the problem becomes a square plate simply supported on four edges. This is evident in the equality of bending moments $(M_x)_{max}$ and $(M_y)_{max}$ in Table 3.1 for $\lambda = \infty$. In Figures 3.8 and 3.9, the two are noticeably different. This is a direct result of the displacement function having a different approximating function in the two different directions, x and y.

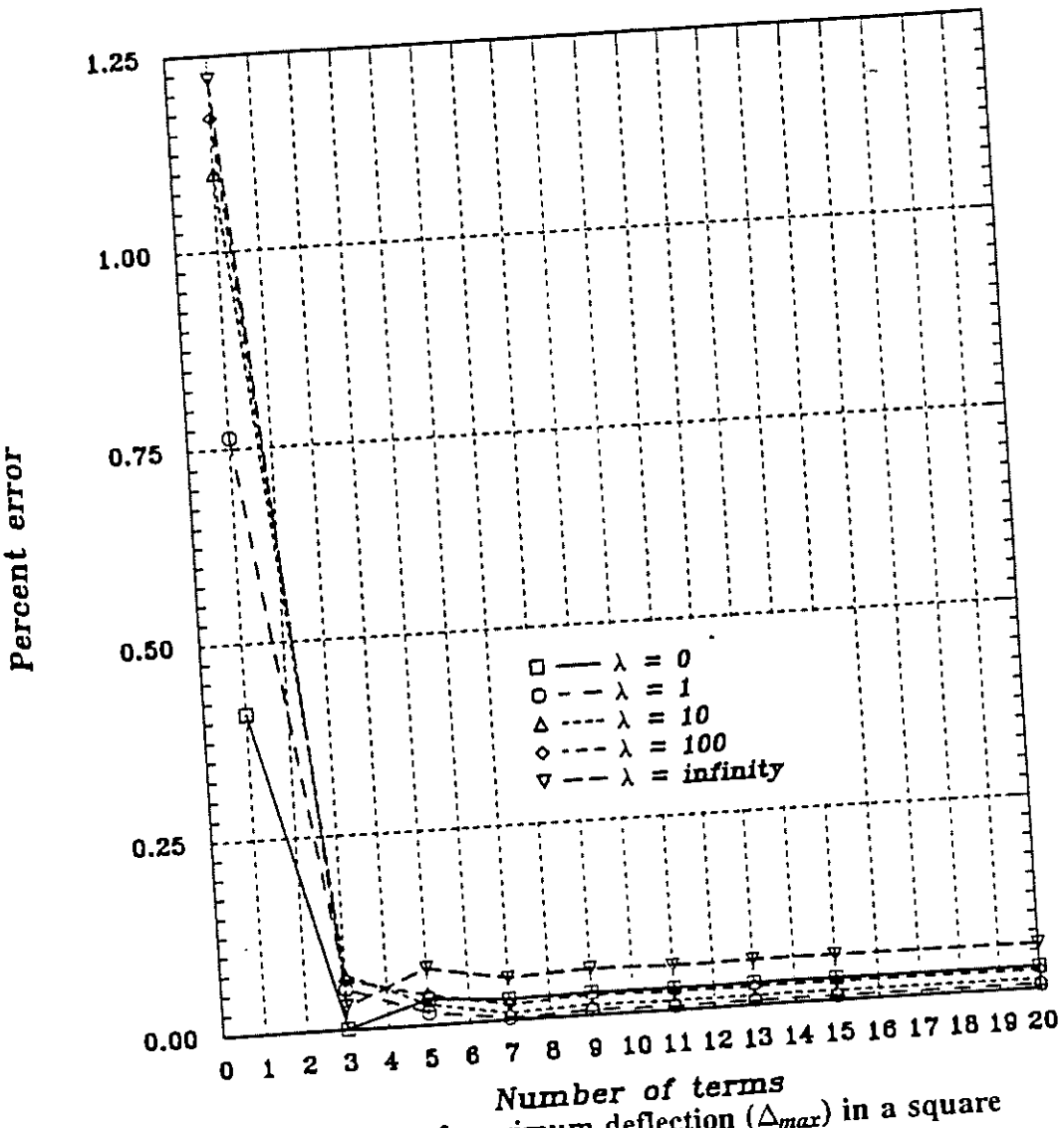

Figure 3.7. Convergence of maximum deflection (Δ_{max}) in a square plate with two edges simply supported and two edges supported with elastic beams.

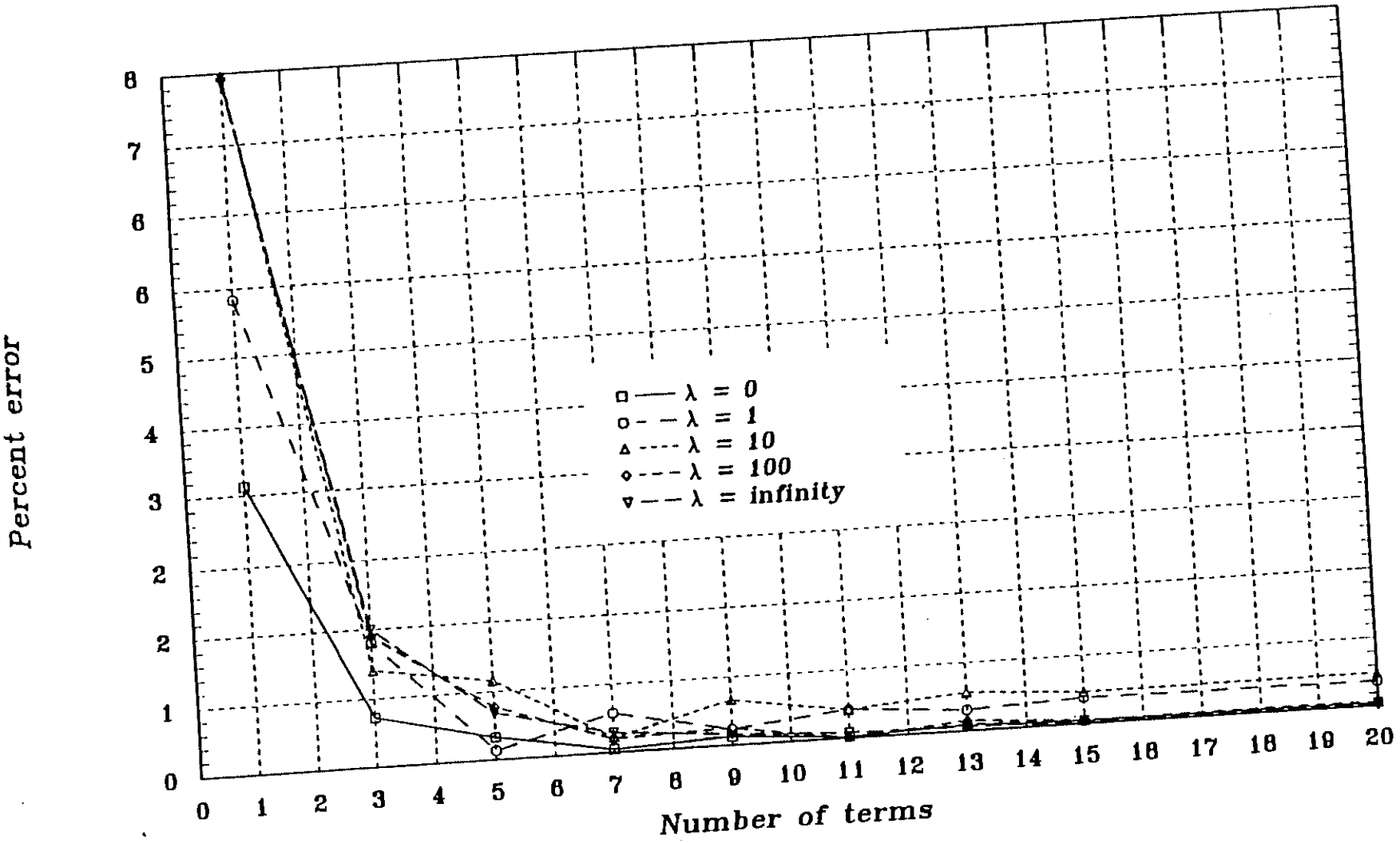

Figure 3.8. Convergence of maximum bending moment $(M_x)_{max}$ in a square plate with two edges simply supported and two edges supported with elastic beams.

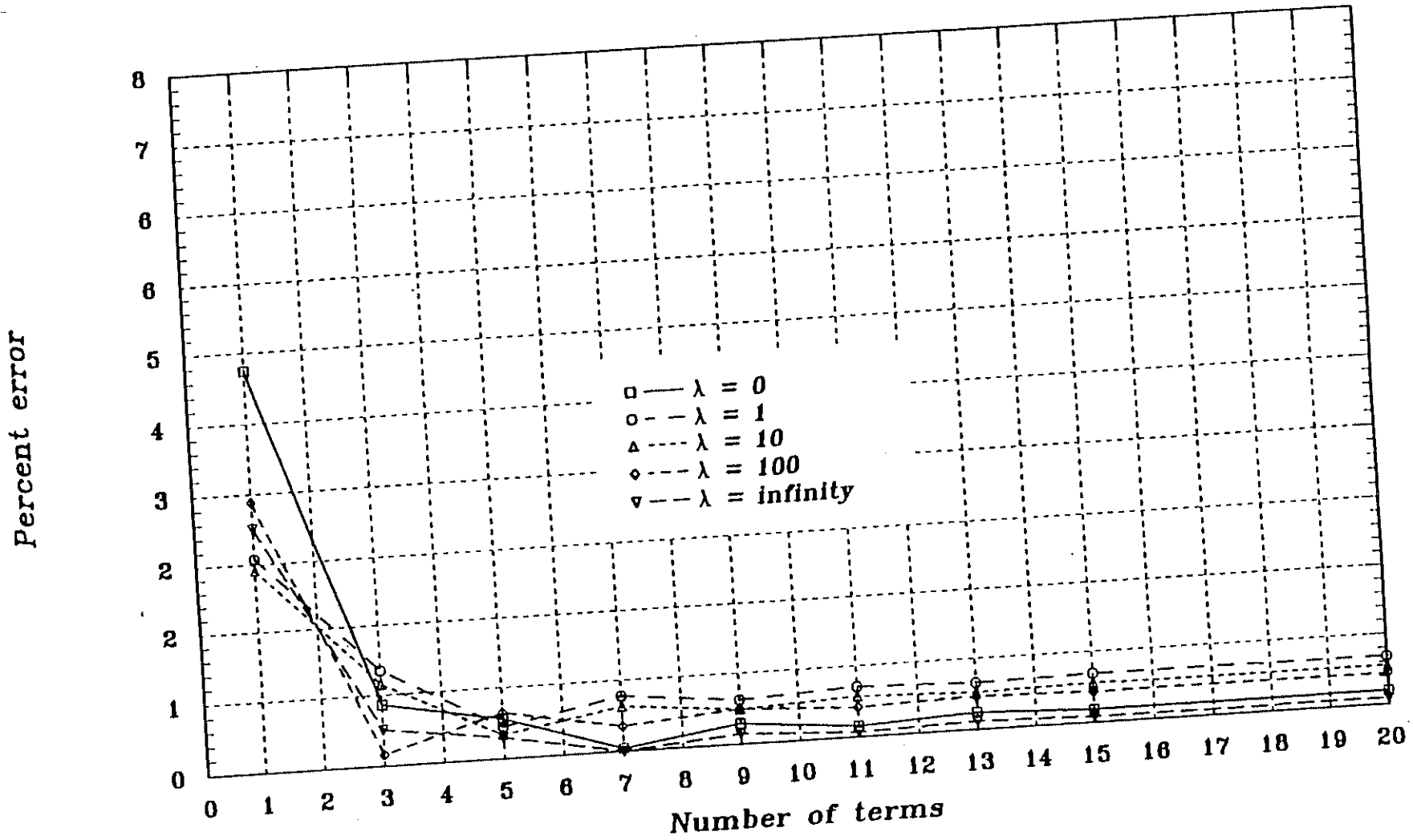

Figure 3.9. Convergence of maximum bending moment $(M_y)_{max}$ in a square plate with two edges simply supported and two edges supported with elastic beams.

3.3. SIMPLY SUPPORTED SINGLE STRIP WITH A CENTRALLY LOCATED BEAM

In order to arrive at the load distribution factor for the individual girders of a bridge, it is necessary to know the response of the bridge to the loads. A verification problem was devised to resemble the actions of the girder in response to a load imposed on the surface of the bridge deck.

As shown in Figure 3.10, an individual finite strip with a longitudinal beam attached at the strip center was used as the test problem. The strip was loaded with a concentrated point load at one quarter span, and the numerical values for deflection (Δ), bending moment (M_x) and shear (V) in the beam were compared to the values obtained from elastic beam theory.

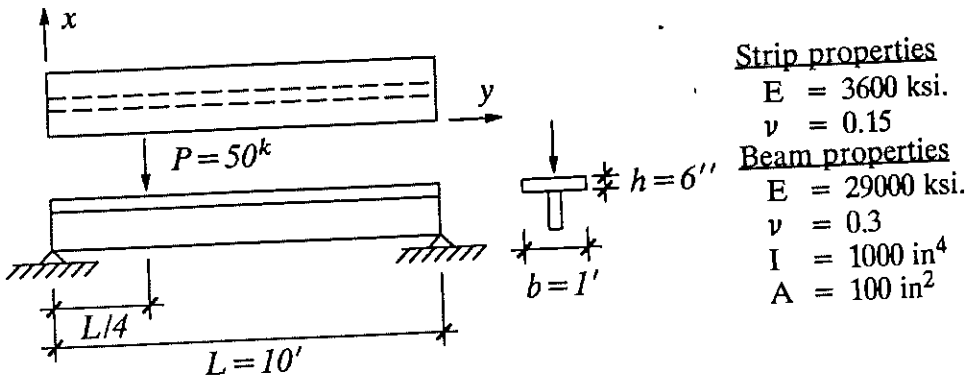

Figure 3.10. Simply supported single strip with a centrally located beam.

The results from the analysis of the problem are presented graphically in Figure 3.11. The deflection along the beam, which corresponds to the deflection along the strip, is determined from equation (2.9) which states

$$w(x,y) = \sum_{m=1}^{r} [N]\{\delta_m\} \sin\frac{m\pi y}{L} \qquad \ldots\ldots\ldots\ldots\ldots\ldots (3.3)$$

where $[N]$ is a matrix containing the shape functions for the strip and $\{\delta_m\}$ contains the various displacement amplitudes for the strip.

Equation (3.3) is the function used to represent the elastic curve of the both the strip and the beam. The second derivative of the function $w(x,y)$ is referred to as the curvature. The bending moment (M_x) in the beam is related to the curvature by

$$M_x = EI\frac{d^2w}{dy^2} \qquad \ldots\ldots\ldots\ldots\ldots\ldots\ldots\ldots (3.4)$$

where EI is the combined flexural rigidity of the strip and the beam. The shear (V) in the beam is related to the third derive of the function $w(x,y)$ by

$$V = EI\frac{d^3w}{dy^3} \qquad \ldots\ldots\ldots\ldots\ldots\ldots\ldots\ldots (3.5)$$

It should be noted that in order to achieve the shear illustrated in Figure 3.11(c) using the FSM, it was necessary to use one hundred terms in the summation. Trying to approximate the shear in the beam with a Fourier series (equation 3.3) poses an interesting problem. Figure 3.12 shows that at points where V is continuous, the partial sums do approach $V(y)$ as m increases. However, in the area of points of discontinuity, directly under the point load, the partial sums do not converge smoothly to the mean value. Instead the partial sums tend to overshoot $V(y)$ at the ends of the jump, as they cannot accommodate the sharp transition at this point. This behavior is typical when using Fourier series to represent points of discontinuity, and is known as the Gibbs phenomenon, named after Josiah Willard Gibbs (1839–1903) (7).

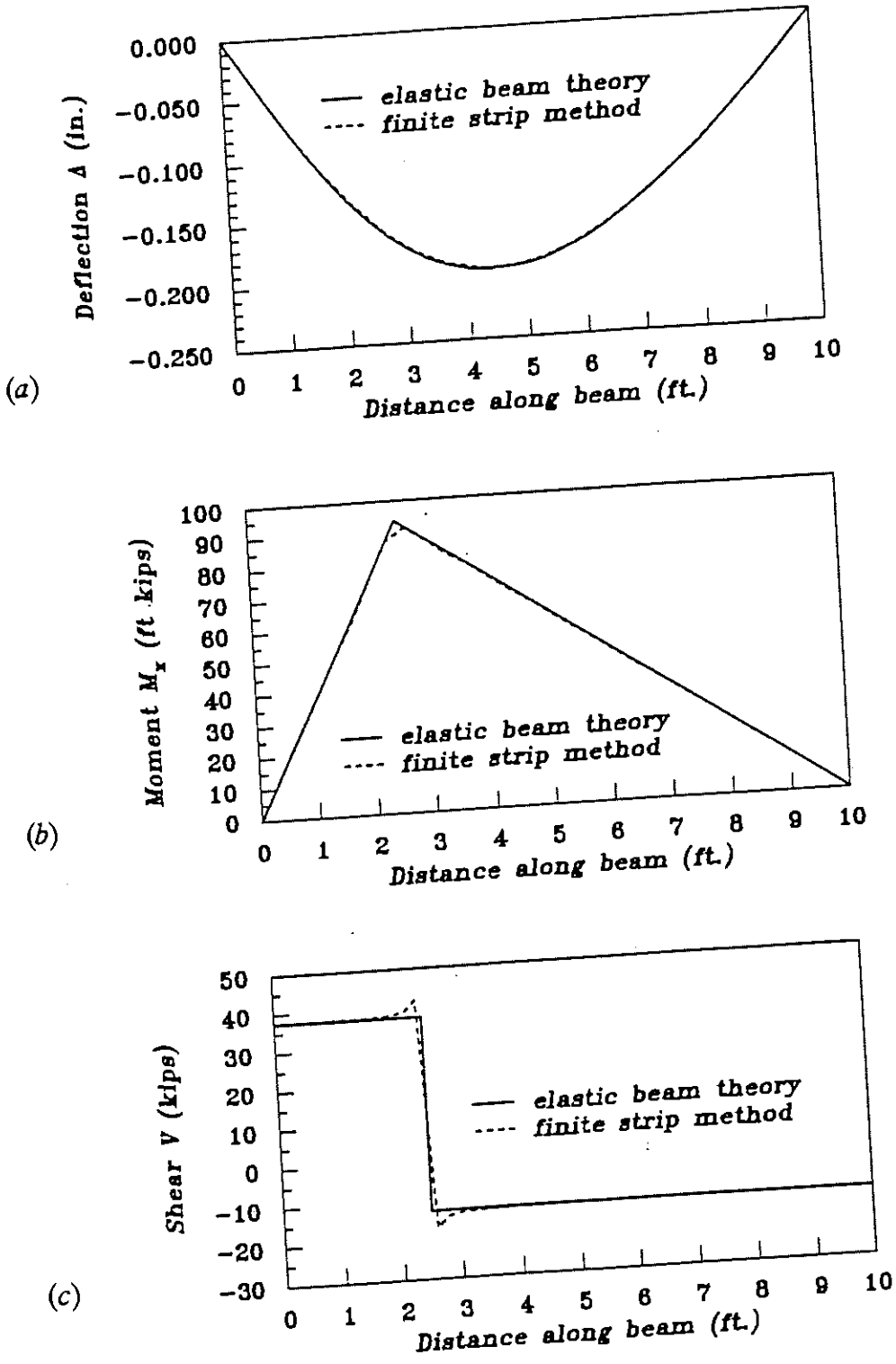

Figure 3.11. Comparison between the finite strip method and elastic beam theory for deflection, moment and shear in a beam.

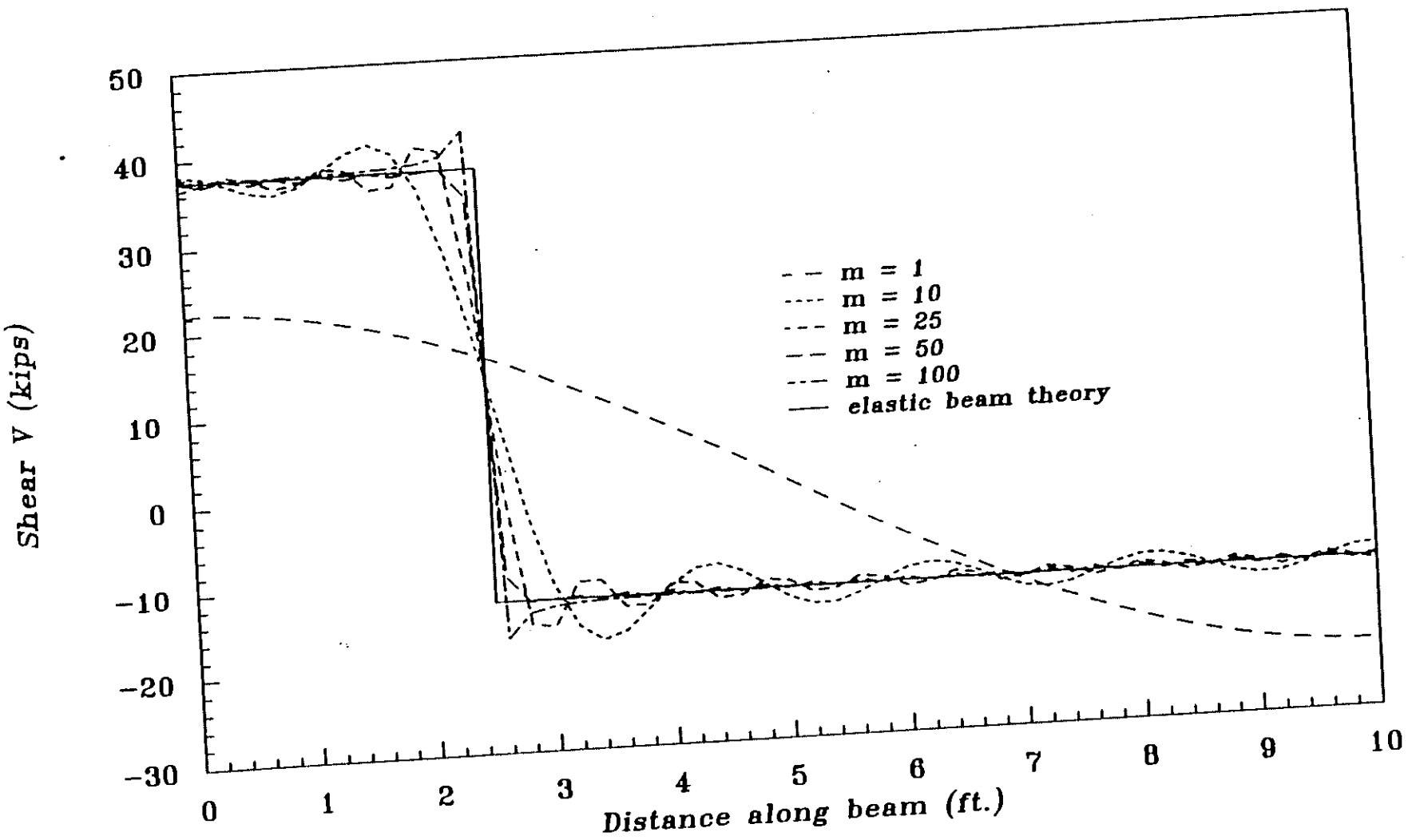

Figure 3.12. Fourier series approximations at a point of discontinuity in beam shear.

3.4. CONVERGENCE OF DISTRIBUTION FACTORS

It was of primary importance to ensure the finite strip method could accurately model a "thin plate" system with elastic supporting elements. A bridge deck supported by girders is an excellent example of this type of "thin plate" system. The response of a bridge deck to a set of loads is difficult to quantify. Thus, it was necessary to be certain that the numerical values obtained by the program had sufficiently converged to the correct solution.

The load distribution factor (*DF*) for any individual girder is determined by

$$DF = \frac{M_{FSM}}{M_{beam}}$$

where M_{FSM} is the moment determined from the finite strip method, and M_{beam} is the moment determined from elastic beam theory assuming the loads to act directly on the girder. It is the moment determined from the finite strip method, M_{FSM}, is considered to be the more accurate representation of the actual moment in the beam. Since M_{FSM} is the only parameter that changes with successive model refinement, the distribution factor *(DF)* converges at the same rate as M_{FSM}. To properly quantify the distribution factors for both moment and shear in the beam, a default of 100 terms with 50 strips was selected.

CHAPTER 4

COMPARISON OF DISTRIBUTION FACTORS FOR AN ILLUSTRATIVE EXAMPLE

The illustrative example used to compare the distribution factors obtained by the methods described in Chapter 1 is shown in Figure 4.1. The example problem is a single span composite bridge composed of a reinforced concrete slab supported by steel girders. The top flanges of the girders are embedded in the concrete slab, and it was assumed that this results in a fully composite flexural response.

4.1. EFFECTS OF SLAB THICKNESS AND SPAN LENGTH

Program BRASS–DIST was used to perform the analysis. BRASS–DIST computes distribution factors for both moment and shear at girder tenth points. The method for determining these distribution factors uses the entire weight of the individual truck axles. The distribution factors for each girder are then multiplied by the gross weight of the truck to determine the distribution of load to a specific girder.

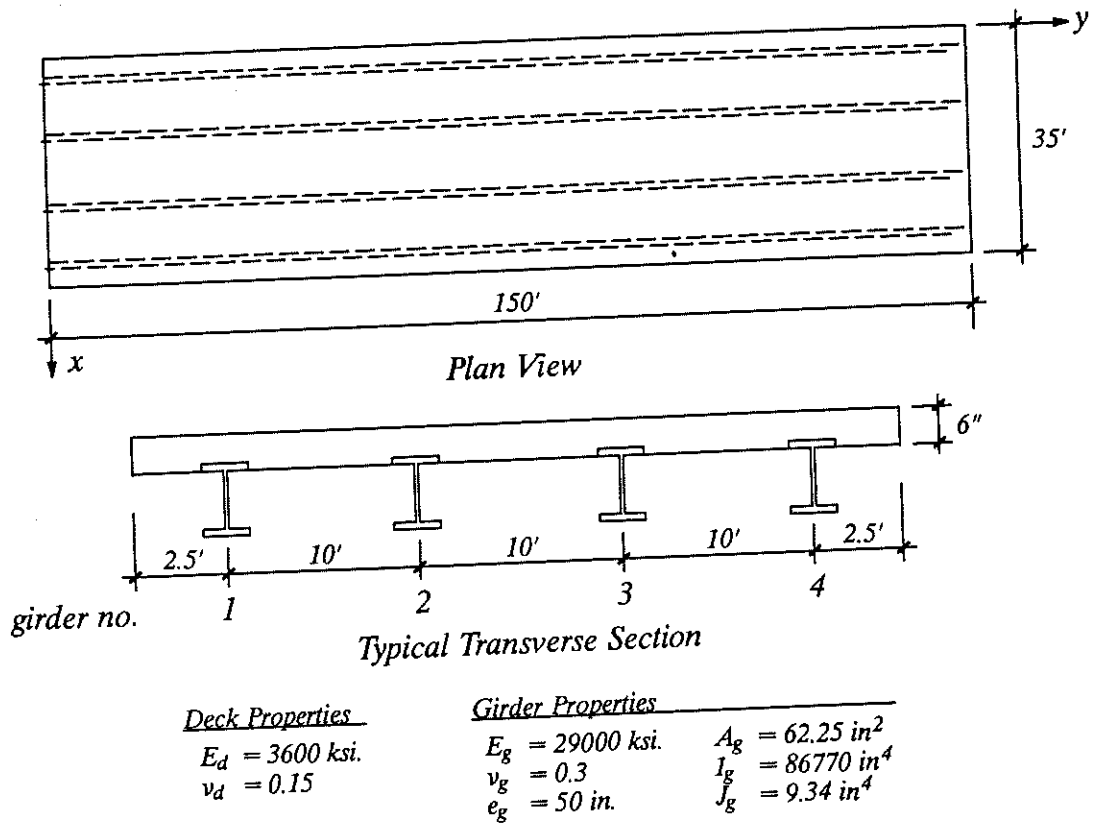

Figure 4.1. Single Span Composite Bridge.

This method differs from the traditional method of load distribution in which the distribution factors are determined from half of the axle weight or wheel line. The method employed by BRASS–DIST was used to accommodate permit vehicles where a single line of wheels cannot by readily defined. *For comparison purposes, the distribution factors obtained by BRASS–DIST have been multiplied by a factor of two in all subsequent graphical representations.* This permits convenient comparisons with traditional methods.

An input file was created for the bridge shown in Figure 4.1, and this file is presented in Appendix B. The structure was loaded with a standard AASHTO HS 20 truck located directly over girder 3 and the rear axle was positioned at a distance $y = 55'$ (refer to Figure

4.2). The thickness of the slab (t_s) was varied from four inches to twelve inches in increments of two inches to illustrate the effects of the relative stiffness of the deck and girders. The results of the analyses are presented in Figure 4.3. Notice that the distribution factor for moment in girder 3 decreases with increasing slab thickness. Intuitively, as the slab thickness increases, the relative stiffness of the slab increases compared to the overall stiffness of the girders. In other words, as the slab thickness increases, the load distributes more evenly to the girders. Notice also in Figure 4.3 that for a slab thickness of four inches, the maximum distribution factor occurs at a distance $y = 60'$, and for a slab thickness of twelve inches, the maximum distribution factor occurs at a distance $y = 75'$. This demonstrates the unpredictable nature of load distribution.

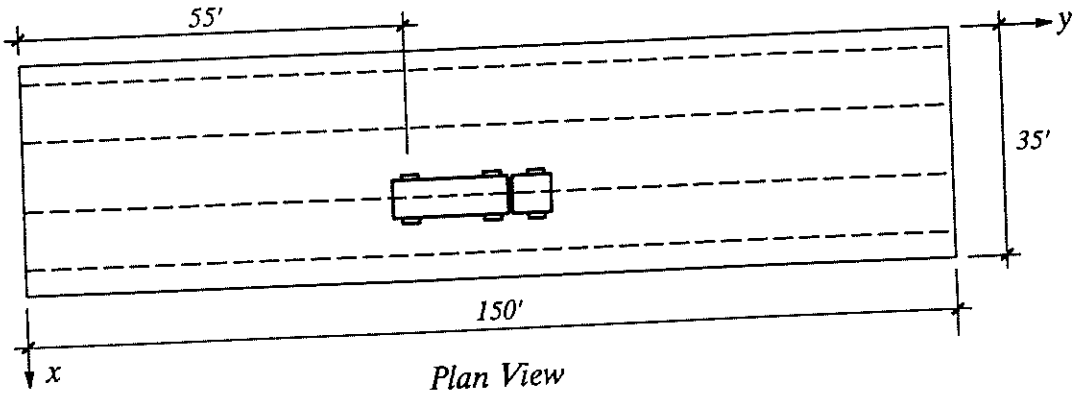

Figure 4.2. Truck Positioning for a Single-lane Loading Case.

In addition to slab thickness, the effect of span length on distribution factors was also studied. The span length of the bridge in Figure 4.1 was varied from 100′ to 200′ by increments of 10′ and the slab thickness was held at six inches. The relative position of the truck with respect to the span length was held constant. The maximum distribution factor for moment in both the interior and exterior girders was determined. The results of these

analyses are presented in Figure 4.4. Notice that the maximum distribution factors for interior girders decrease with increasing span length while the maximum distribution factors for exterior girders increase with increasing span length. This relationship indicates that, for this particular bridge, as the span length increases, the slab becomes stiffer compared to the girders and better load distribution is achieved.

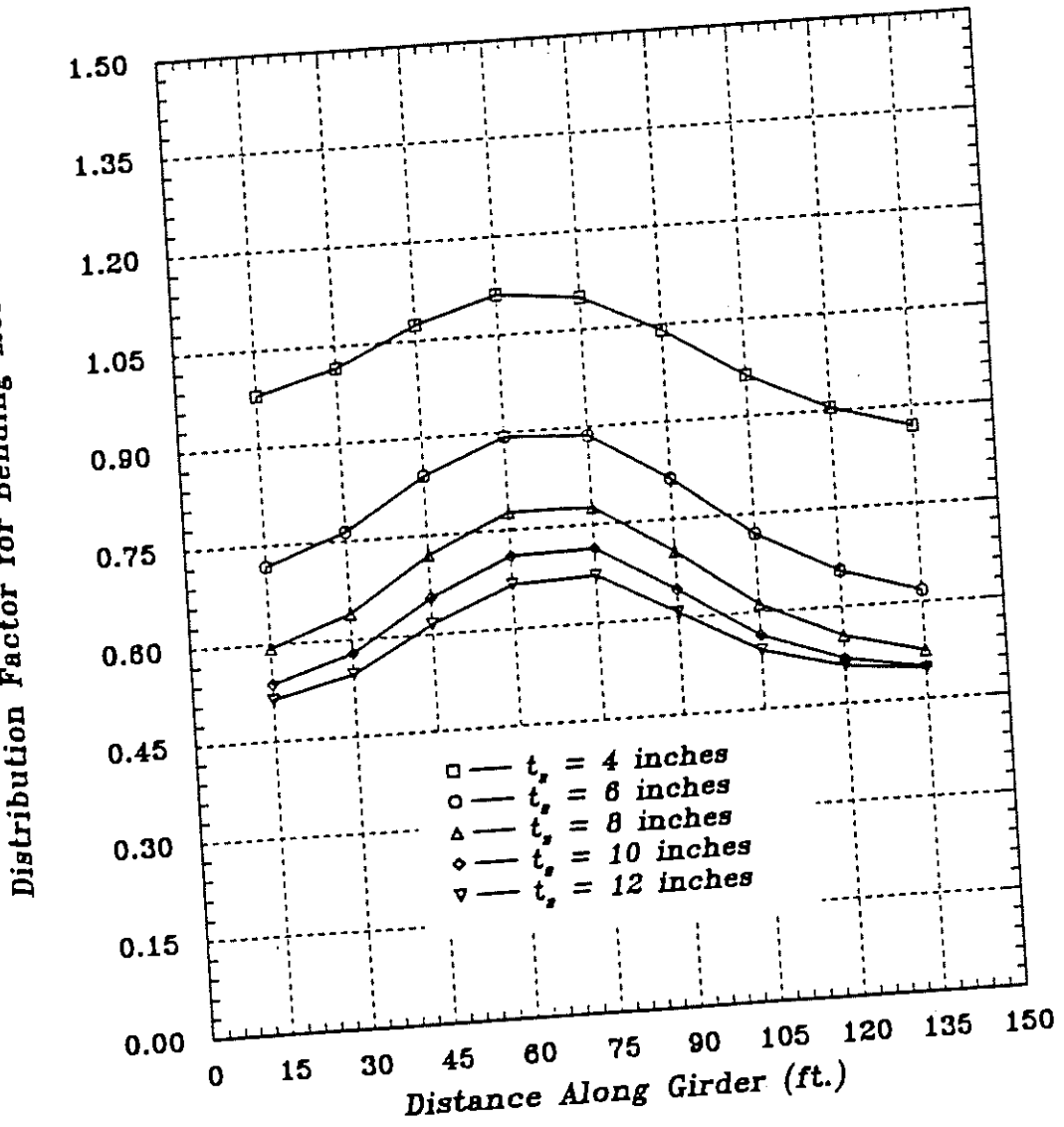

Figure 4.3. Effects of Slab Thickness on Distribution Factors for Moment.

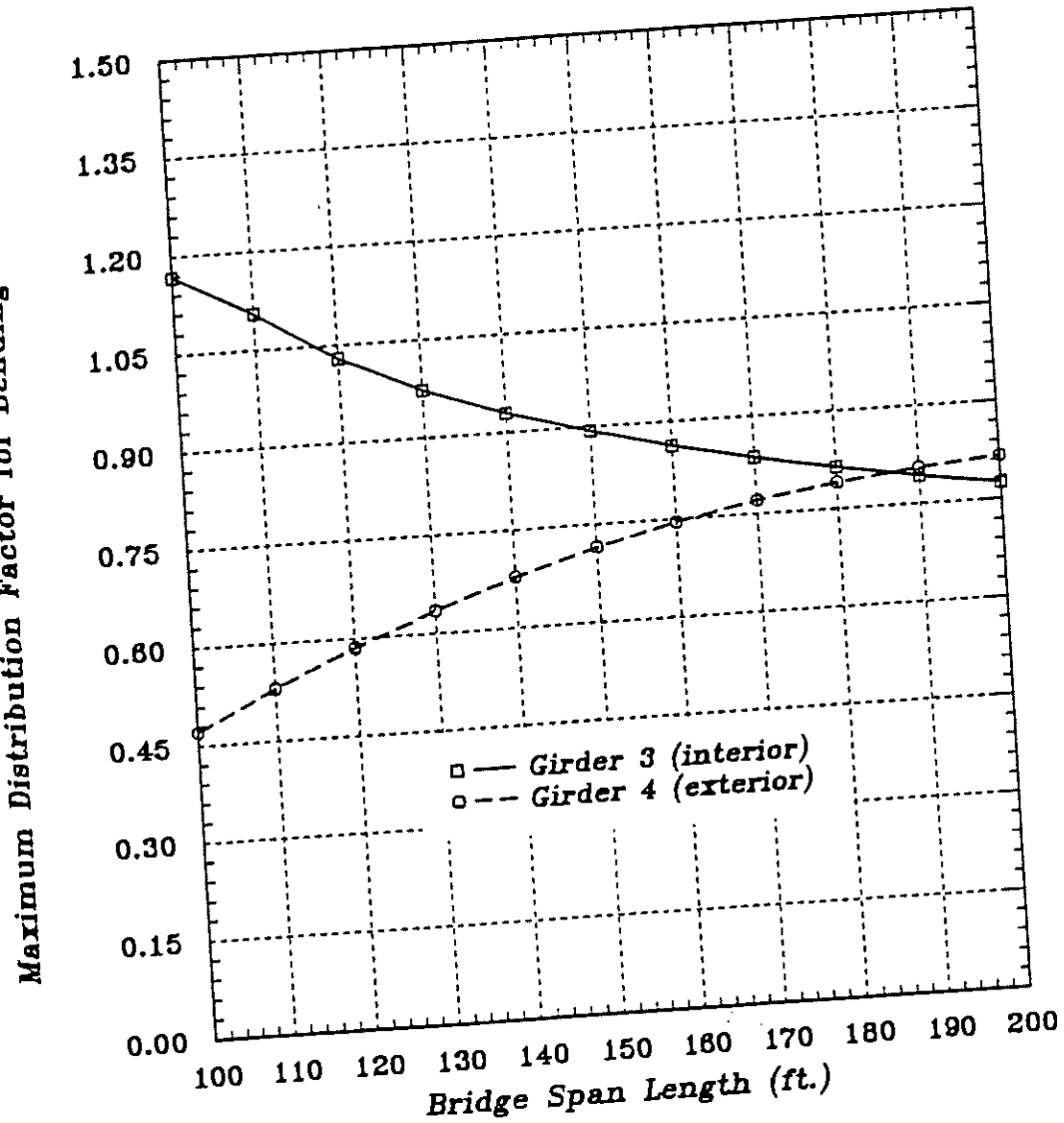

Figure 4.4. Effects of Span Length on Maximum Distribution Factor for Moment.

4.2. EFFECTS OF SINGLE AND MULTIPLE LANE LOADING

The effects of lane loading on distribution factors is of great importance. Recall that in the AASHTO method of load distribution, the distribution factor for slab–girder bridges is $S/7.0$ for one traffic lane and $S/5.5$ for two or more traffic lanes. The Ontario Highway Bridge Design Code (*17*) accounts for the number of loaded lanes by providing separate design charts for one, two, three and four lane bridges. In the simplified methods developed by NCHRP project 12–26 (*12*), two different sets of equations exist for determining distribution factors, one for single–lane loading and one for multi–lane loading.

The bridge in Figure 4.1 was used to compare distribution factors obtained by BRASS–DIST to those obtained by various simplified methods. The first comparison was made for the single lane loading case. A standard AASHTO HS 20 truck was positioned directly over girder 3 at a distance $y=55'$ (refer to Figure 4.2). The results obtained by BRASS–DIST were compared to the AASHTO and NCHRP project 12–26 methods. These results are presented in Figure 4.5. It is important to note that the AASHTO method does not distinguish between interior and exterior girders in the determination of its distribution factors. This feature increases the degree of conservatism of an already conservative method.

There are very few simplified methods for determining distribution factors for single lane loading. Most of the developments in recent years have been devoted to the multi–lane loading case. To simulate a multi–lane loaded bridge, two standard AASHTO HS 20 trucks were superimposed on the bridge as shown in Figure 4.6. This load case was analyzed with BRASS–DIST and the results were compared to various other simplified methods. A

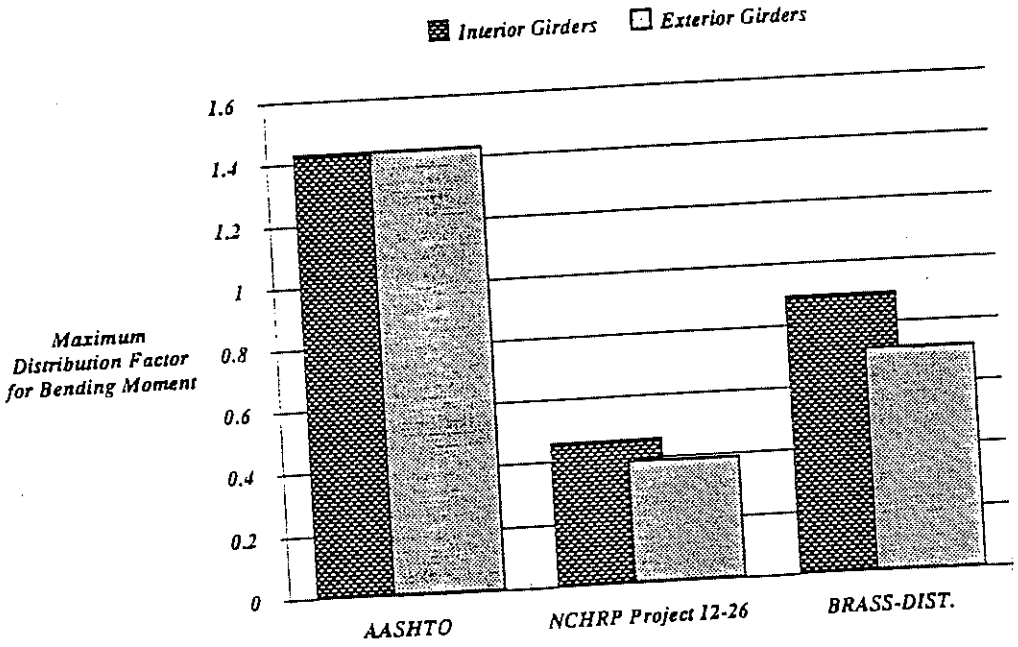

Figure 4.5. Comparison of Maximum Distribution Factors for Moment for the Single–lane Loading Case.

compilation of the results obtained from these methods is presented in Figure 4.7. In comparing the various methods, the degree of conservatism for each method can be determined. The numerical values for almost every method are below those of AASHTO's, with the exception of Tarhini and Frederick (*23*) and Marx, et al. (*15*). It was observed during the literature review that the simplified formula developed by Tarhini and Frederick (*23*) did not specify an upper sound on the span length. As part of their investigation they considered

span lengths up to 119'. This may be a contributing factor to the overconservative nature of this simplified formula. It should be stated that average distribution factor for moment as determined from the simplified method developed by NCHRP project 12–26 (equation 1.3) was 1.378. This average number was determined from the parametric studies performed on all of the slab–girder bridges contained in the NCHRP database.

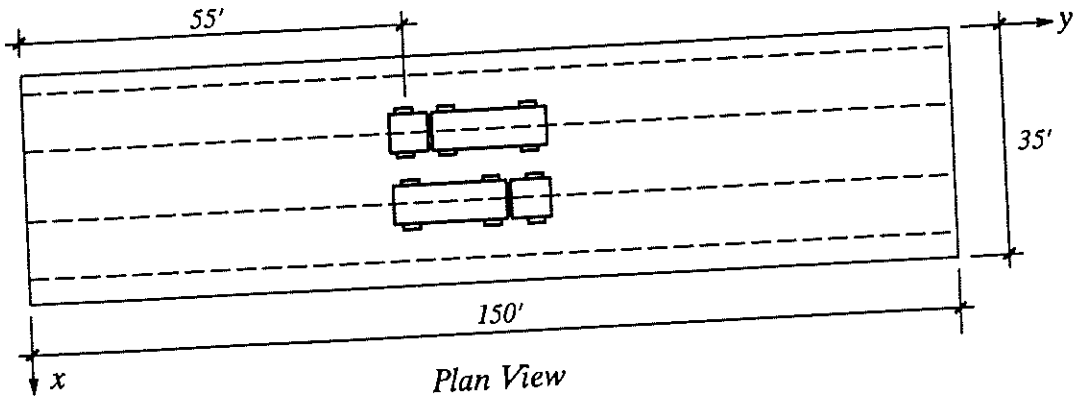

Figure 4.6. Truck Positioning for a Multi–lane Loading Case.

A second method of comparing distribution factors was also used . This method involved varying the girder spacing. Girder spacing is the one variable common to all the simplified methods for determining distribution factors. The relationship between maximum distribution factor for moment and girder spacing for the various methods is presented in Figure 4.8. Notice that the AASHTO method has the largest slope, or largest rate of increase for distribution factor. This is another example of the oversimplistic representation of the AASHTO method.

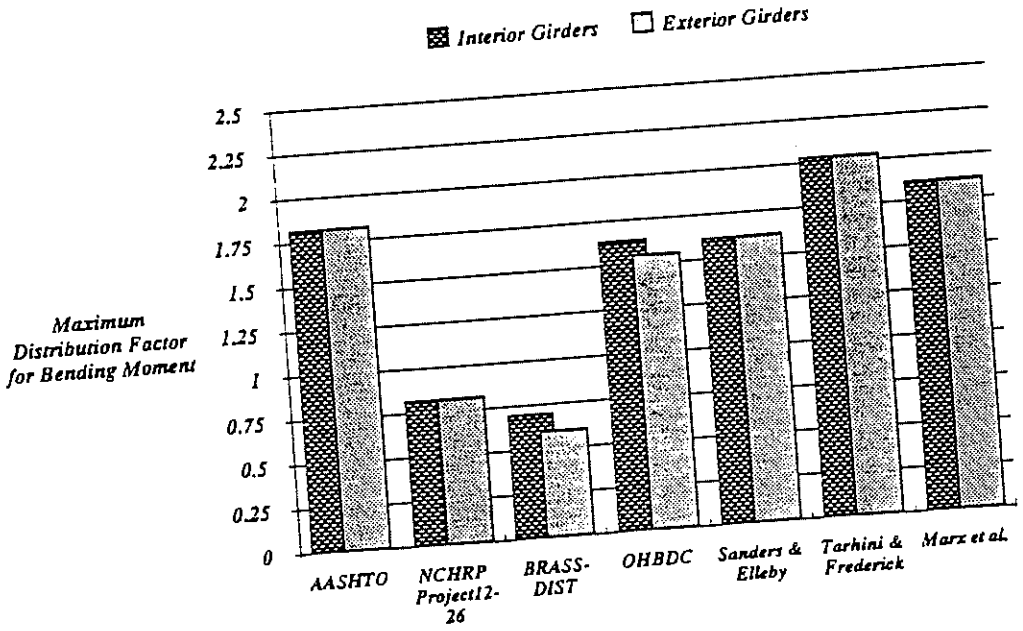

Figure 4.7. Comparison of Maximum Distribution Factors for Moment for the Multi-lane Loading Case.

Previous to NCHRP project 12-26, no research has been devoted to the development of a simplified formula for determining distribution factors for shear in the girders of highway bridges. Equations (1.6) and (1.8) were developed specifically for this purpose. A comparison between BRASS-DIST and these two equations for the illustrative example is presented in Figure 4.9.

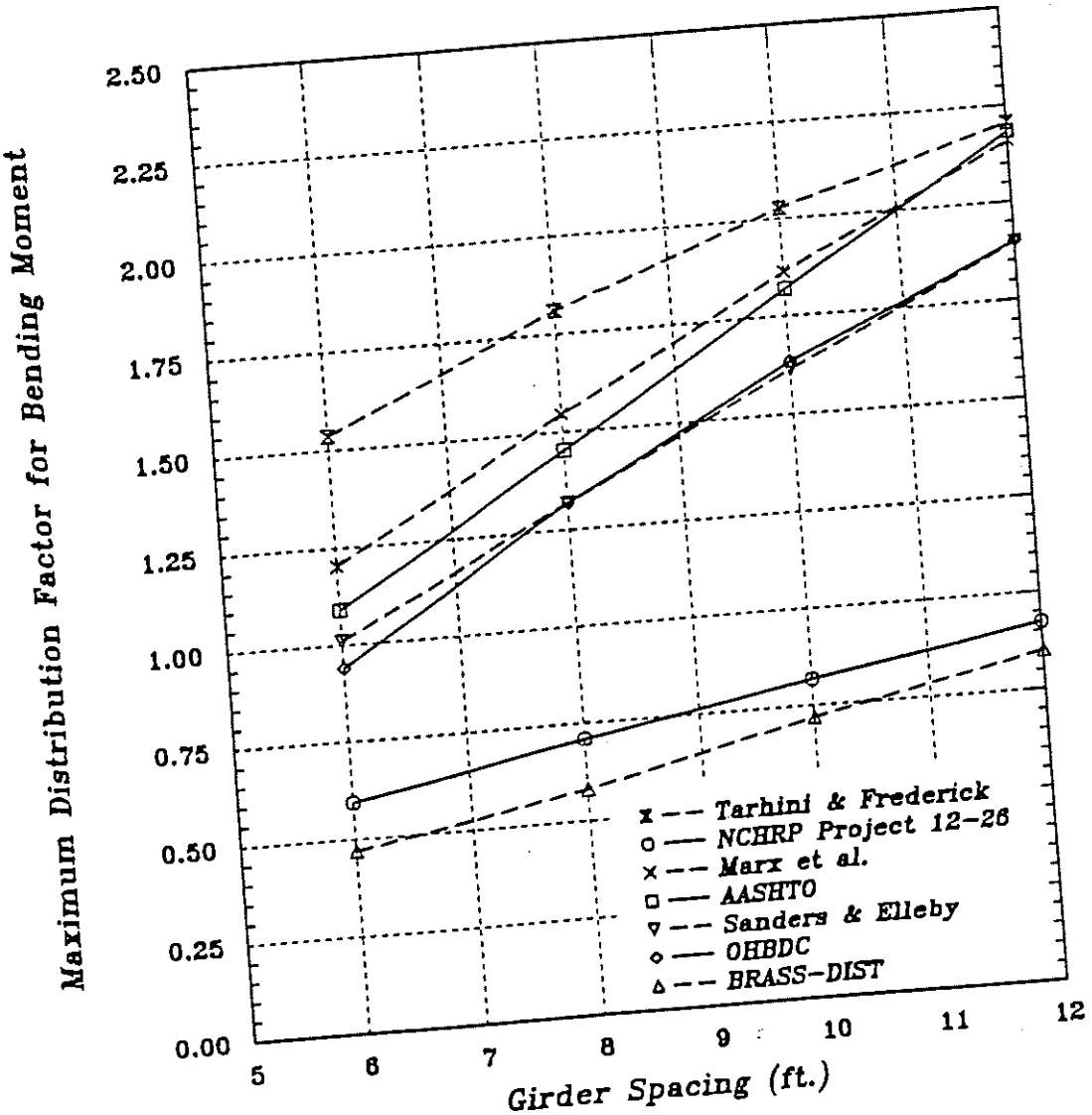

Figure 4.8. Effects of Girder Spacing on Maximum Distribution Factors for Moment.

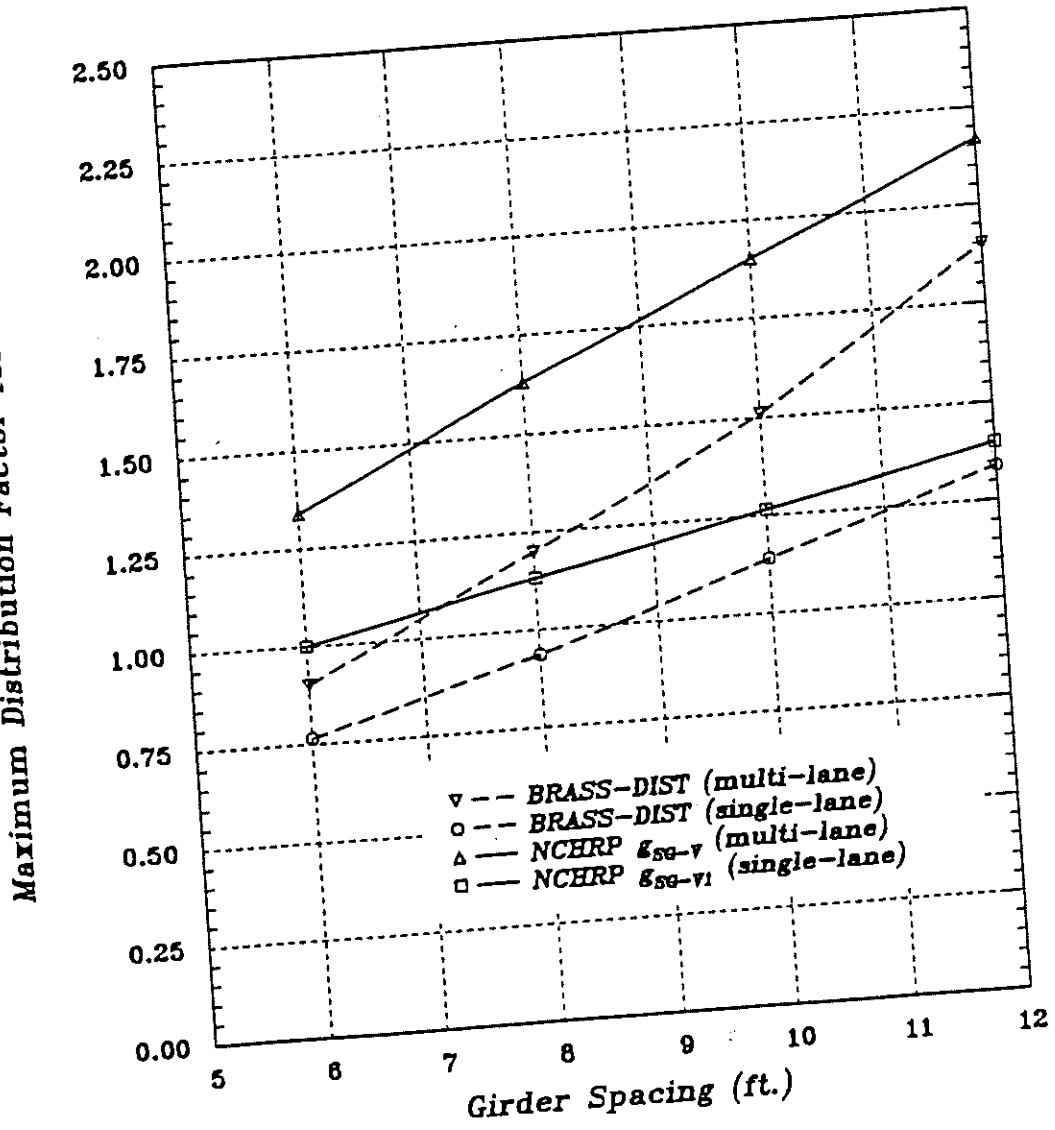

Figure 4.9. Effects of Girder Spacing on Maximum Distribution Factors for Shear.

4.3. DISTRIBUTION FACTORS FOR A PERMIT VEHICLE

The formulae developed in NCHRP project 12–26 were based on the standard AASHTO "HS" family of trucks. In a limited parametric study it was concluded that variations in the truck axle configuration or truck weight did not significantly effect the distribution factors (*12*). It was also recommended that with some caution these formulae could be applied to "other" trucks.

One of the main reasons for developing BRASS–DIST was to be able to quantify distribution factors for permit–type vehicles with irregular axle configurations. An actual permit vehicle that was encountered by the Wyoming Department of Transportation was an MX transporter with a stage I missile on carriages. The axle configuration and load distribution for this vehicle is shown in Figure 4.10.

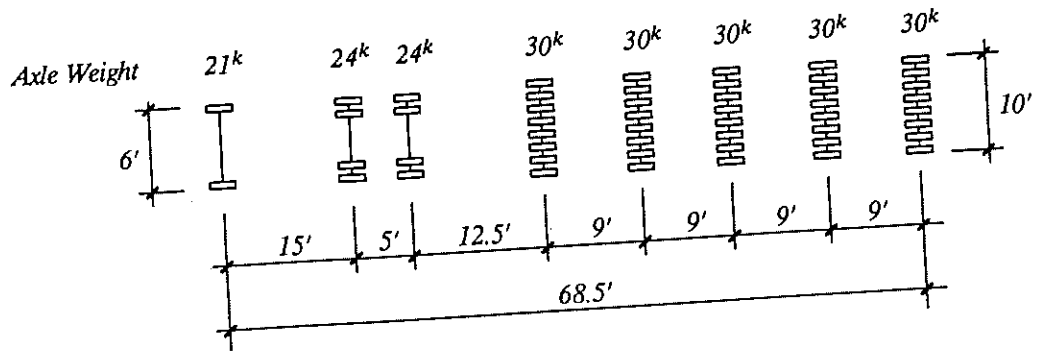

Figure 4.10. Axle Configuration and Load Distribution for an MX Transporter.

This vehicle was modeled on the composite bridge in Figure 4.1. The vehicle was centered on the bridge width and the rear axle was positioned at a distance $y = 40'$. Due to the symmetry of both load and structure at $x = 17.5'$, only the distribution factors for girders 3 and 4 were calculated. The results of the BRASS–DIST analysis are presented in Figure 4.11. Girder 3 is an interior girder which attracts more of the load than an exterior girder.

This is becomes evident by comparing the distribution factors for girders 3 and 4. It is interesting to note that the location of the maximum distribution factor for both moment and shear varies with the girder position. Further, the sum of the factors for the interior and exterior girders is unity, indicating that 100 percent of the wheel line load is carried by these two elements. In other words, this is a check on equilibrium.

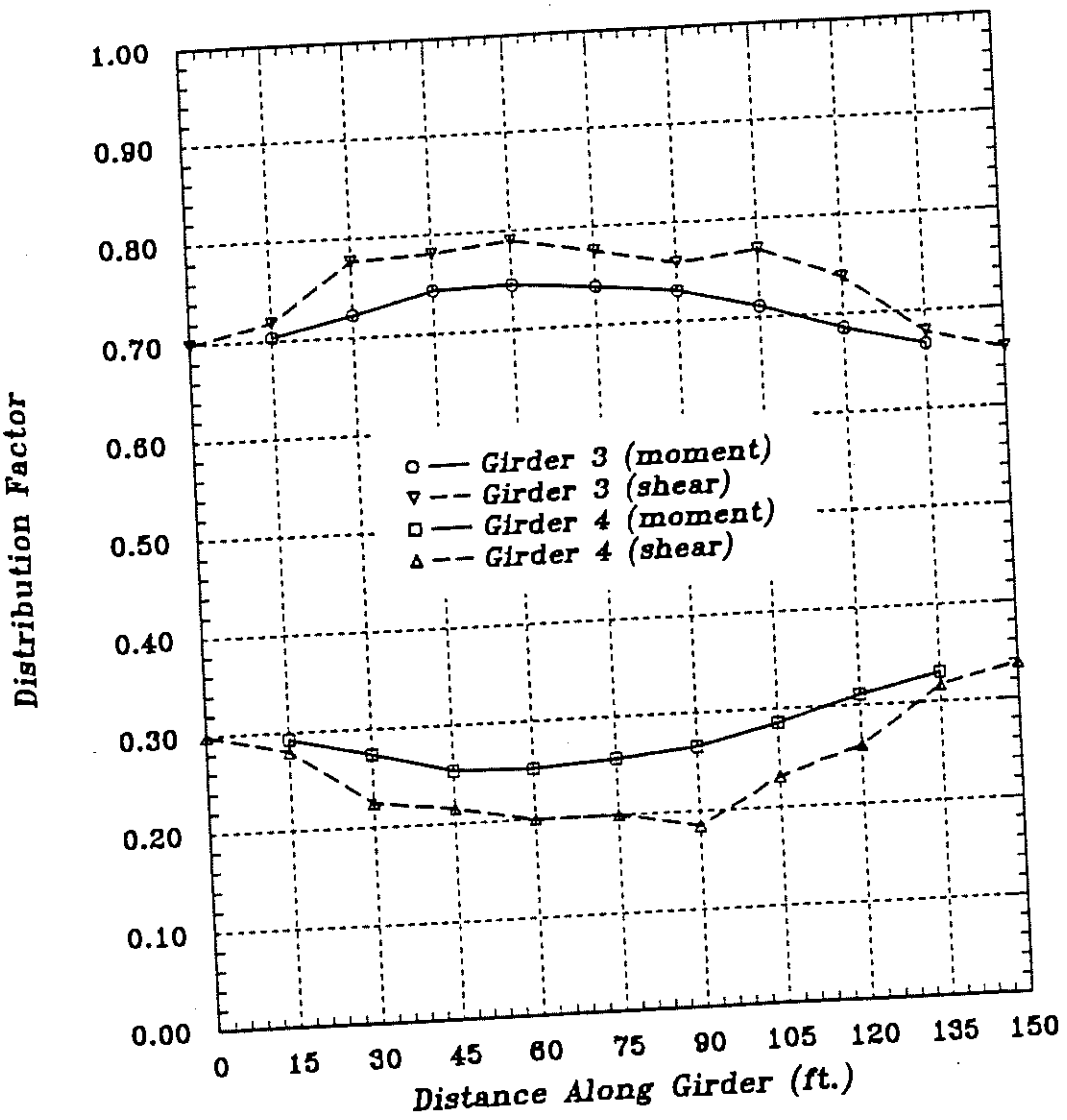

Figure 4.11. Distribution Factors for Moment and Shear for an MX Transporter.

CHAPTER 5

SUMMARY AND CONCLUSIONS

5.1. SUMMARY

There are several simplified methods available for determining distribution factors for the girders of highway bridges. These methods differ in the number of parameters used to define a bridge and its properties, and in their ease of use. While the AASHTO method, for example, is extremely easy to use, it has been determined that this method is too simplistic and cannot account for all the aspects of a bridge influening its load distribution characteristics. The objective of this research was to develop an automated procedure for accurately determining distribution factors.

The finite strip method proved to be a valuable tool in the development of an automated procedure for determining the distribution factors on highway bridges. The fact that typically a highway bridge has regular geometry and continuous boundary conditions, was the main reason for selecting the FSM as the modeling procedure. In Chapter 3 it was demonstrated that various solution parameters responded differently to the number of terms

included in the summations and the number of strips used to discretize the bridge deck. Several verification problems were used to test solution convergence to correct values established from elastic beam theory and the theory of plates and shells. Once convergence had been established for all of the solution parameters, the corresponding numbers of strips and terms were used as the default parameters in the BRASS–DIST program. In addition to verifying convergence of solution parameters, every effort was made to check both global and element equilibrium where appropriate. This was done to check the various loading routines and the superposition of different loading routines.

Once all of the convergence tests were performed on BRASS–DIST, the program was used to model an actual highway bridge subjected to truck loading. Several parameters were varied to further understand the sensitivity of distribution factors to both the geometric characteristics of the bridge and the magnitude and location of the loads.

5.2. CONCLUSIONS

The overconservative nature of the AASHTO method of load distribution was demonstrated by several of the comparisons discussed in Chapter 4. Because of the extensive research conducted in NCHRP project 12–26 (finite element modeling, compilation of a database of actual bridges, parametric studies and statistical analyses), it was assumed that these equations could accurately determine the distribution factors to the girders of a slab–on–girder bridge. In all the comparisons made for the illustrative example, it was observed that the distribution factors obtained by BRASS–DIST were slightly below those obtained by the simplified formulae developed by NCHRP project 12–26. As part of the literature review, it was determined that the simplified formulae given in NCHRP project

12–26 (*12*) were developed using variational methods and were then modified to assure slightly conservative results. It should be noted that the distribution factors obtained by BRASS–DIST are also slightly conservative because of the original simply–supported assumption.

In comparing the various simplified methods for determining distribution factors, the simplicity of use for each method was also evaluated. The results of this evaluation in order of increasing complexity of use is given below

- AASHTO (*22*)
- Tarhini and Frederick (*23*)
- NCHRP project 12–26 (*12*)
- Marx et al. (*15*)
- Sanders and Elleby (*23*)
- OHBDC (*17*)

The Ontario Highway Bridge Design Code (OHBDC) method of load distribution was the most difficult to use. The method requires the calculation of longitudinal and transverse flexural and torsional equivalent plate properties. A set of dimensionless characterizing parameters are determined from the equivalent plate properties. Numerical values are determined from design charts with the characterizing parameters, and these numerical values are used in a simplified formula to determine the distribution factor.

The method developed by Sanders and Elleby (*23*) is the next most difficult to use. The difficulty arises in the calculation of an individual stiffness parameter requiring numerical values for both the moment of inertia and the torsional constant about two axes for a composite member.

Similar to Sanders and Elleby, the method developed by Marx et al. (*15*) requires the calculation of a flexural slab stiffness parameter, but it is not based on a composite member, which simplifies the calculations.

The simplified formulae developed in NCHRP project 12–26 (*21*) were found to be relatively simple to use. The equation parameters consist of quantities that are familiar to a bridge engineer such as girder spacing, span length, deck thickness, girder moment of inertia, girder cross sectional area, and girder eccentricity.

Both the AASHTO method and the method developed by Tarhini and Frederick (*23*) are very simple to use. The AASHTO method is based on girder spacing and the number of traffic lanes, and the method developed by Tarhini and Frederick is dependent on girder spacing and span length.

It is important to note that the comparison of distribution factors presented in Chapter 4 is applicable only to the bridge in Figure 4.1, and does not in general apply to similar bridge types. One of the most important distinctions that should be made is that the distribution of load in a highway bridge is a function of the magnitude and location of the loads and the response of the particular bridge to these loads.

5.3. RECOMMENDATIONS FOR FUTURE RESEARCH

In the development of BRASS–DIST it was assumed that the bridge had a simply supported boundary condition on both ends. The next logical step for improving BRASS–DIST would be the inclusion of several boundary conditions, the most important of which being the fixed–fixed condition and the fixed–pinned condition. The actual boundary conditions for a bridge are neither pinned–pinned nor fixed–fixed, but are somewhere

between the two. By analyzing the same bridge with these two different boundary conditions, an upper and lower bounds could be placed on the distribution factors, and it would be left to the discretion of the bridge engineer to estimate the amount of rotational stiffness provided by the bridge to get an accurate assessment of the distribution factors. The fixed–fixed boundary condition would be extremely helpful in the evaluation of a single span of a two span bridge. This particular boundary condition would more accurately represent the behavior of a two span bridge with an interior support.

The series formulations for the two boundary conditions mentioned above were included in Chapter 2 (equations 2.13 and 2.14). To incorporate these additional boundary conditions into BRASS–DIST, it would be necessary to rewrite the equation solver. Currently for a model containing n nodes, in which m terms are to be considered in the summation, the m sets of n nodal parameters for each term are solved separately and then superimposed. For the added boundary conditions, the integrations required for the strip stiffness matrices do not uncouple. This requires the simultaneous solution of m x n sets of parameters. For a typical model with 50 strips and 100 terms, there are 51 nodal lines with 4 degrees of freedom per line and 100 terms. This system contains over 20,000 degrees of freedom that would need to be solved simultaneously.

Another limitation of BRASS–DIST is that it can only analyze bridges that are rectangular in plan. In order to accommodate bridges that are curved in plan, a coordinate transformation would be required for the finite strip method. This adaptation is handled quite easily in the FSM. Almost of the formulations for transforming a rectangular

coordinate system (x and y) to a polar coordinate system (r and θ) are given in *Finite Strip Method in Structural Analysis (8)*. Once this coordinate transformation is made, the geometry of a curved bridge could be specified in terms of its radial lines r and the angle θ that it sweeps.

In addition to curved bridges, modern construction also requires some bridges have skewed supports. Transformations for both interior and exterior skewed supports are also given in *Finite Strip Method in Structural Analysis (8)*. With these modifications, BRASS–DIST would become a very versatile program, as there are no simplified methods for determining distribution factors for highway bridges that are curved in plan, or have with skewed supports.

APPENDIX A

COMPUTER ALGORITHM

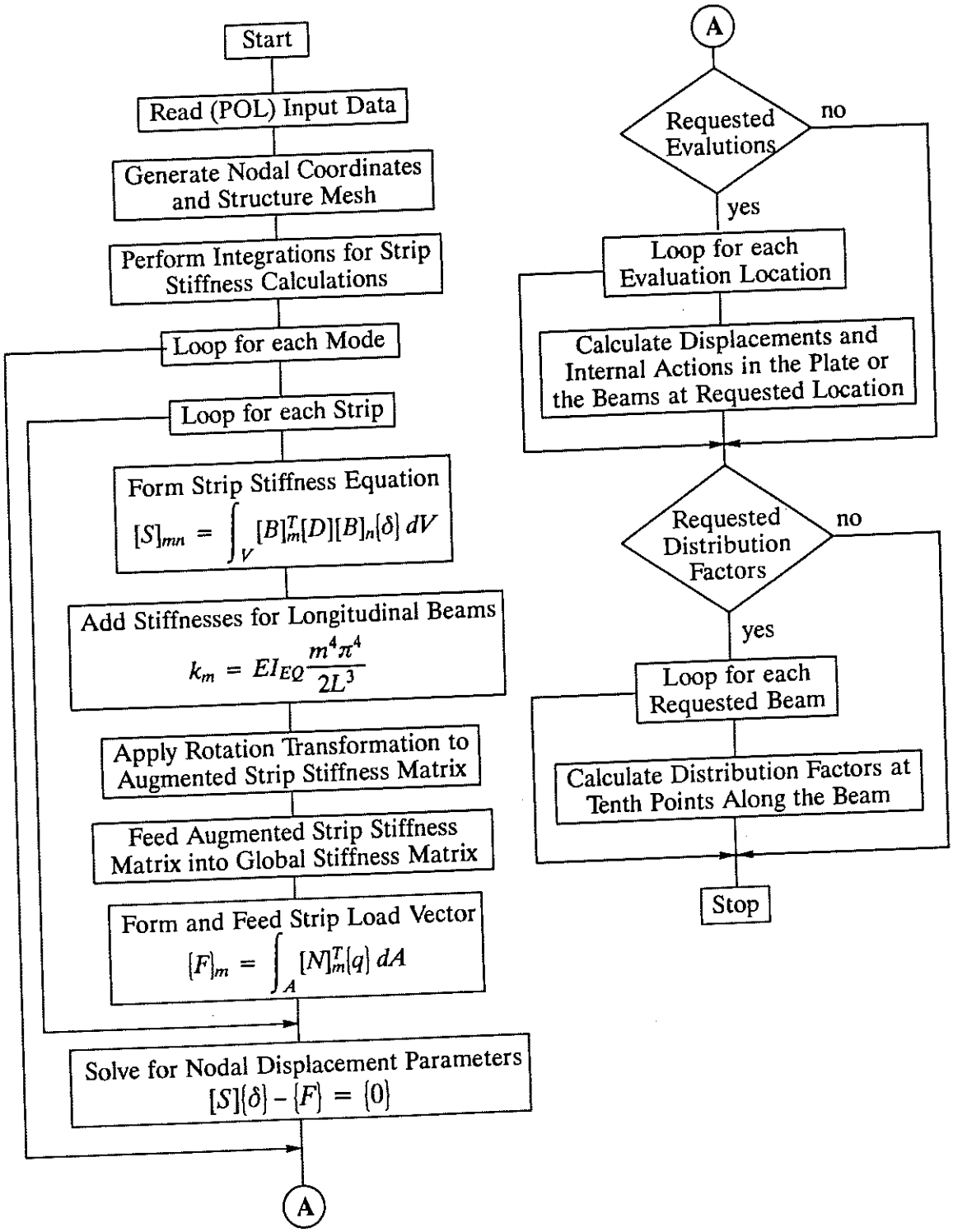

Figure A.1. Sequence of operations in the finite strip computer algorithm.

APPENDIX B

BRASS-DISTRIBUTION FACTOR DOCUMENTATION

The software documentation for BRASS-DIST consists of a set of command descriptions for each command including command name, purpose, command parameters, and example and any figures applicable to the command.

The command name is a six character string that defines the data that proceeds it. Typically the meaning is determined from context. The typical format for an individual command is

COMMAND DATA, DATA, DATA, DATA

An example command file for a single span composite bridge supported with four girders and loaded with an AASHTO HS-20 truck is given below.

```
TITLE   EXAMPLE COMMAND FILE
OUTPUT  1, 0
GEOMET  150, 35
DCKPRP  3600, 3600, 0.15, 0.15, 6, 0.15
GRDMAT  29000, 0.3, 0.490
GRDPRP  50, 62.25, 86770, 9.34, 2.5
GRDPRP  50, 62.25, 86770, 9.34, 9
GRDPRP  50, 62.25, 86770, 9.34, 9
GRDPRP  50, 62.25, 86770, 9.34, 9
TRUCKP  1, 19.5, 55
TRUCKL  1, 3, 6, 0, 32, 6, 20, 32, 6, 14, 8
GIRDEV  3, 1, 1, 1, 1
```

10	BRASS	COMMAND DESCRIPTION
COMMAND NAME	TITLE	
PURPOSE	This command is used to give a project a specific title.	

COMMAND PARAMETERS	
TITLE	Enter the job title

EXAMPLE

TITLE Job number 4

FIGURES

NOTES

20	BRASS	COMMAND DESCRIPTION
COMMAND NAME	COMMENT	
PURPOSE	This command is used to place a comment in the input file.	

COMMAND PARAMETERS	
COMM	Enter the comment

EXAMPLE

COMMENT Have a nice day!

FIGURES

NOTES

30	BRASS	COMMAND DESCRIPTION

COMMAND NAME	OUTPUT
PURPOSE	This command is used to control the amount of output provided by the program.

COMMAND PARAMETERS

ISOD	Output of distribution factors (S over D ratios) toggle (0 – off 1 – on)
IFWRIT	Full output of program information including individual strip properties and calculated constants. toggle (0 – off 1 – on)

EXAMPLE

OUTPUT 1, 1

FIGURES

NOTES

40	BRASS	COMMAND DESCRIPTION
COMMAND NAME	GEOMET	
PURPOSE	This command is used to set the geometry of the bridge.	

COMMAND PARAMETERS

ALEN	Enter the bridge span length, feet.
BW	Enter the width of the bridge, feet.

EXAMPLE

GEOMET 40, 20

FIGURES

NOTES

50	BRASS	COMMAND DESCRIPTION
COMMAND NAME	GRDMAT	
PURPOSE	This command is used to set the girder material properties. The specified material properties are used for all girders.	

COMMAND PARAMETERS

GIRDE	Enter the girder modulus of elasticity (E), ksi.
GIRDV	Enter Poisson's ratio (ν) for the girder, dimensionless.
GIRDD	Enter the girder density, kcf.

EXAMPLE

```
GRDMAT    29000, 0.3, 0.4
```

FIGURES

NOTES

60	BRASS	COMMAND DESCRIPTION

COMMAND NAME	GRDPRP
PURPOSE	This command is used to set the cross sectional properties for each individual girder. Note: Each girder requires a command.

COMMAND PARAMETERS

GIRDEC	Enter the girder eccentricity from the centriod of the deck to the centriod of the girder in inches. See figure.
GIRDA	Enter the cross sectional area (A) of the girder, in^2.
GIRDI	Enter the moment of inertia (I) of the girder, in^4.
GIRDJ	Enter the torsional constant (J) of the girder, in^4.
GIRDS	Enter the center to center distance from the left adjacent girder (or edge) in feet. See figure.

EXAMPLE

GRDPRP 9, 8.84, 170, 0.62, 1 (for the left girder)

–and–

GRDPRP 9, 8.84, 170, 0.62, 2 (for the right girder)

FIGURES

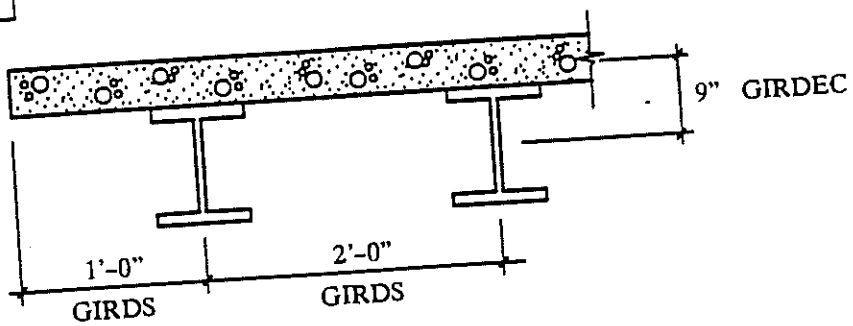

NOTES

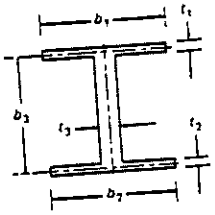

$$J = \frac{b_1 t_1^3 + b_2 t_2^3 + b_3 t_3^3}{3}$$

70	BRASS	COMMAND DESCRIPTION

COMMAND NAME	DCKPRP
PURPOSE	This command is used to set the properties for the deck, and the boundary conditions for the bridge.

COMMAND PARAMETERS

EX	Enter the modulus of elasticity for the deck in the X direction, ksi. See figure.
EY	Enter the modulus of elasticity for the deck in the Y direction, ksi. See figure.
VX	Enter Poisson's ratio for the deck in the X direction, dimensionless. See figure.
VY	Enter Poisson's ratio for the deck in the Y direction, dimensionless. See figure.
TT	Enter the deck thickness, inches.
DEN	Enter the density of the deck, kcf.

EXAMPLE

```
DCKPRP    3600, 3600, 0.15, 0.15, 6, 0.150
```

FIGURES

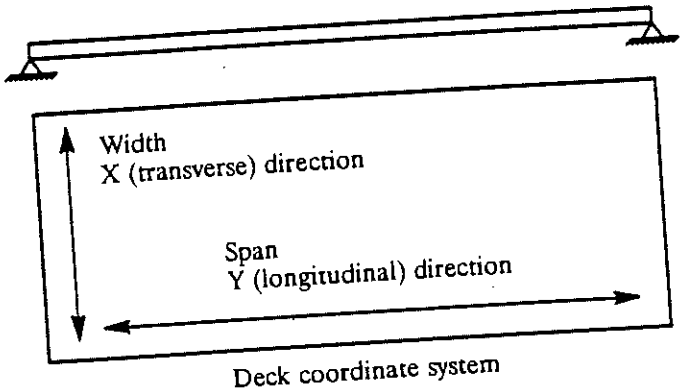

Deck coordinate system

NOTES

80	BRASS	COMMAND DESCRIPTION
COMMAND NAME	UNIFML	
PURPOSE	This command is used to impose a uniform area load over the entire deck. A maximum of 1 load may be entered.	

COMMAND PARAMETERS	
Q1	Enter the magnitude of the uniform area load, ksf.

EXAMPLE

```
UNIFML    100
```

FIGURES

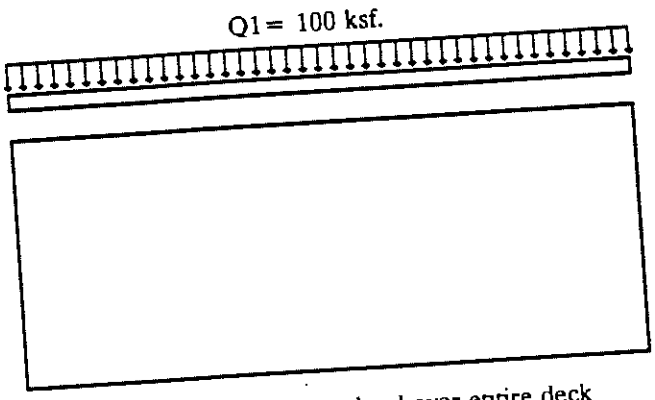

Imposed uniform area load over entire deck

NOTES

90	BRASS	COMMAND DESCRIPTION
COMMAND NAME	PATCHL	
PURPOSE	This command is used to impose a uniform patch load on the deck.	

COMMAND PARAMETERS

QP0	Enter the magnitude of the uniform patch load, ksf.
XP1	Enter the starting X location of the uniform patch load, feet. See figure.
YP1	Enter the starting Y location of the uniform patch load, feet. See figure.
XP2	Enter the ending X location of the uniform patch load, feet. See figure.
YP2	Enter the ending Y location of the uniform patch load, feet. See figure.

EXAMPLE

PATCHL 100, 5, 20, 15, 30

FIGURES

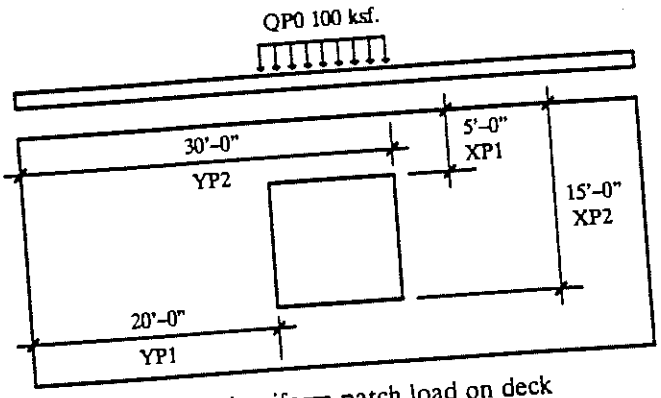

Imposed uniform patch load on deck

NOTES

This command could be used to model curb loads.

100 BRASS	COMMAND DESCRIPTION
COMMAND NAME	POINTL
PURPOSE	This command is used to impose a concentrated point load on the deck.

COMMAND PARAMETERS

PNTL	Enter the magnitude of the concentrated point load, kips.
PNTLX	Enter the X location of the concentrated point load, feet. See figure.
PNTLY	Enter the Y location of the concentrated point load, feet. See figure.

EXAMPLE

POINTL 5, 10, 25

FIGURES

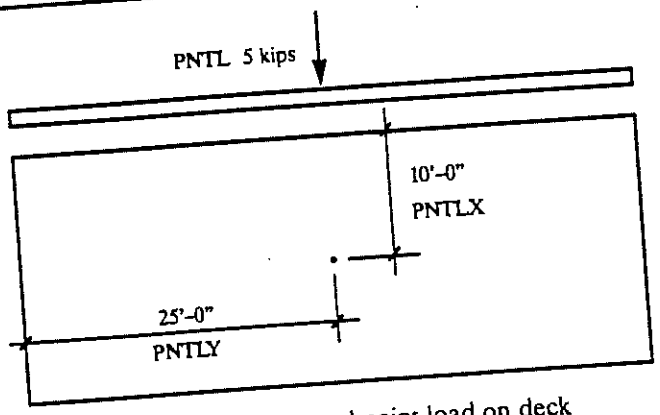

Imposed concentrated point load on deck

NOTES

110 BRASS	COMMAND DESCRIPTION
COMMAND NAME	TRUCKP
PURPOSE	This command is used to position a truck on the bridge.

COMMAND PARAMETERS

ITRKNO	Enter the truck number to be positioned.
TRKX	Enter the X location of the left rear axle of the truck, feet. See figure.
TRKY	Enter the Y location of the rear axle of the truck, feet. See figure.
	Note: One TRUCKP command is required for each truck.

EXAMPLE

TRUCKP 1, 6, 10

FIGURES

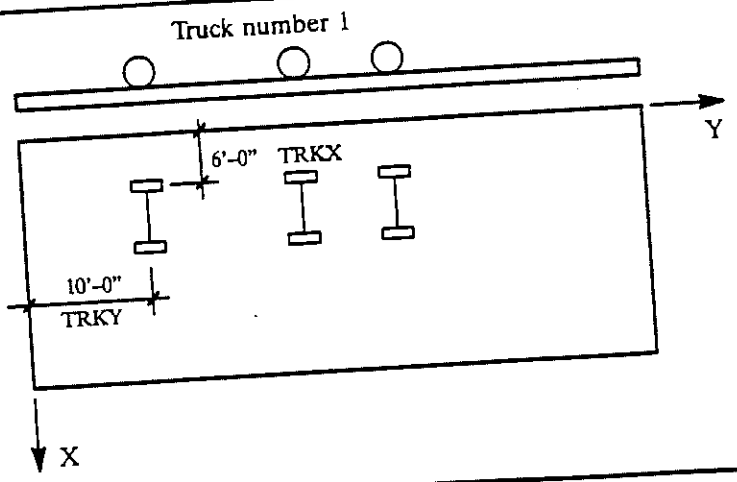

NOTES

120	BRASS	COMMAND DESCRIPTION

COMMAND NAME	TRUCKL
PURPOSE	This command is used to define a typical axle configuration, where there are two wheels per axle.

COMMAND PARAMETERS

ITRKNO	Enter the truck number used to identify the individual truck.
NAXLE	Enter the number of truck axles.
XDIS	Enter the width of each individual truck axle, feet. See figure.
YDIS	Enter the longitudinal location of each individual truck axle with respect to the previous axle, feet. See figure.
WAXLE	Enter the weight of each individual truck axle, kips. See figure.
	Repeat XDIS, YDIS, and WAXLE as necessary.
	Maximum number of axles is twenty.
	Maximum number of trucks is ten.

EXAMPLE

TRUCKP 10, 30

TRUCKL 1, 3, 6, 0, 32, 6, 20, 32, 6, 14, 8

(axle 1: 6, 0, 32; axle 2: 6, 20, 32; axle 3: 6, 14, 8)

FIGURES

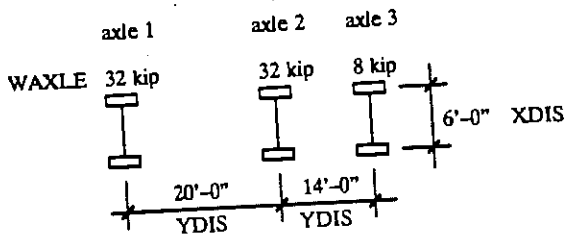

Typical HS-20 truck load

NOTES

Note: The value of YDIS for axle 1 is equal to zero

Note: TRUCKP command positions the truck on the bridge.

130 BRASS	COMMAND DESCRIPTION
COMMAND NAME	TRUCKT
PURPOSE	This command is used to define a permit vehicle that has non-standard axles. Note: One command is required for each axle.

COMMAND PARAMETERS

ITRKNO	Enter the truck number used to identify the individual truck.
NAXLE	Enter the axle number to be defined.
WAXLE	Enter the total weight of the axle, kips. See figure.
YDIS	Enter the longitudinal location of the axle referenced from the previous rear axle, feet. See figure.
NTIRES	Enter the number of wheels in the axle.
XDIS	Enter the width of the axle, feet. See figure.
IWT	Flag for assigning percent load to each wheel (0 – equal distribution of axle weight to uniformly spaced wheels) (1 – varying distribution of axle weight to wheels)
XTDIS (if needed)	Enter the distance from the previous left wheel, feet. See figure.
TFAC (if needed)	Enter the percent of total axle load to be distributed to the wheel. See figure.
	Repeat command as necessary.

EXAMPLE

TRUCKP 10, 30

TRUCKT 1, 1, 40, 0, 4, 8, 0 (for axle 1)

–and–

wheel number: 1 2 3 4

TRUCKT 1, 2, 40, 35, 4, 8, 1, 0, 0.1, 1, 0.4, 6, 0.4, 1, 0.1 (for axle 2)

FIGURES

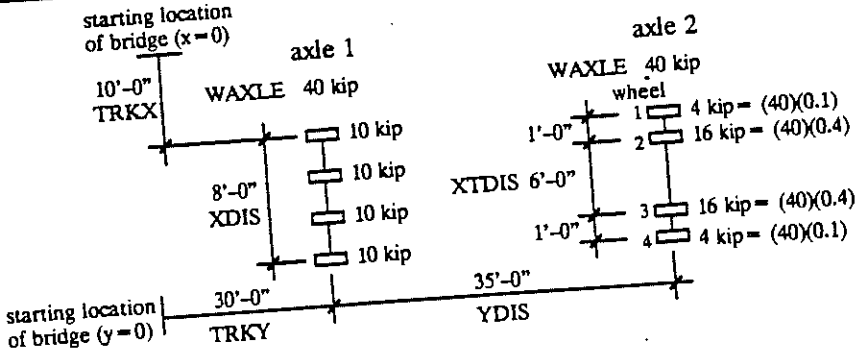

NOTES

Note: The value of YDIS for axle 1 is equal to zero

Note: TRUCKP command positions the truck on the bridge.

140	BRASS	COMMAND DESCRIPTION
COMMAND NAME	EVALPT	
PURPOSE	This command is used to set the location of an evaluation point in the deck.	

COMMAND PARAMETERS

EPGX	Enter the X location of the evaluation point, feet.
EPGY	Enter the Y location of the evaluation point, feet. Note: Not required for girders.

EXAMPLE

EVALPT 10, 25

FIGURES

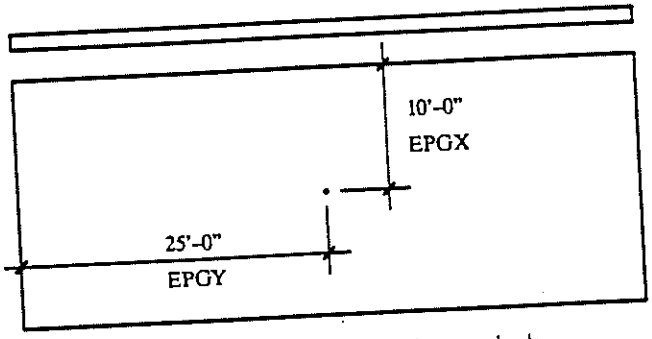

Location of evaluation point on deck

NOTES

150	BRASS	COMMAND DESCRIPTION

COMMAND NAME	EVLINE
PURPOSE	This command is used to set the location of a longitudinal evaluation line in the deck in which tenth points are evaluated.

COMMAND PARAMETERS

XGLIN	Enter the X location of the evaluation line, feet. Note: Not required for girders.

EXAMPLE

EVLINE 10

FIGURES

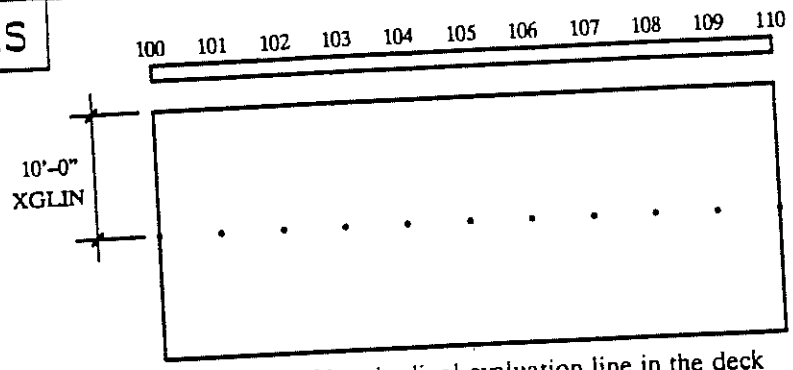

Location of longitudinal evaluation line in the deck

NOTES

160	BRASS	COMMAND DESCRIPTION
COMMAND NAME	GIRDEV	
PURPOSE	This command is used to retrieve both girder actions and distribution factors for shear and moment at tenth points.	

COMMAND PARAMETERS

IGEVAL	Enter the girder number to be evaluated.
ITRUCK	Enter the truck number to be used for evaluation.
IGSOD	Flag for calculation of distribution factors (S over D ratios) toggle (0–off 1–on)
IV	Flag for calculation of shear S over D ratios toggle (0–off 1–on)
IM	Flag for calculation of moment S over D ratios toggle (0–off 1–on)

ENDNOTES

1. Bathe, K., Wilson, E. L., and Peterson, F. E., "SAP IV, A Structural Analysis Program for Static and Dynamic Response of Linear Systems," Report no. EERC 73-11, University of California, Berkeley, CA, (1974).

2. Bakht, B., Cheung, M. S., and Aziz, T., "Application of a Simplified Method of Calculating Longitudinal Moments to the Ontario Highway Bridge Design Code," *Canadian Journal of Civil Engineering*, Vol. 6, No. 1, (1979): 36-50.

3. Bakht, B., and Jaeger, L. G., *Bridge Analysis Simplified*, McGraw-Hill, New York, NY, (1985).

4. Bakht, B., and Jaeger, L. G., "Effect of Vehicle eccentricity on longitudinal moment in bridges," *Canadian Journal of Civil Engineering*, Vol. 10, No. 4, (1983): 582-599.

5. Bakht, B., and Moses, F., "Lateral Distribution Factors for Highway Bridges," *Journal of the Structural Division*, American Society of Civil Engineers, Vol. 114, No. ST 8 (1988): 1785-1803.

6. *Bridge Rating and Analysis of Structural Systems*, Wyoming Highway Department, Report No. FHWA-RD-73-501 & 502, (1980).

7. Carslaw, H. S., *Introduction to the Theory of Fourier's Series and Integrals*, 3rd ed., Cambridge University Press, Cambridge, (1930); reprinted by Dover, New York, NY, (1952).

8. Cheung, Y. K., *Finite Strip Method in Structural Analysis*, Pergamon Press, Oxford, (1976).

9. Cook, R. D., Malkus, D. S., and Plesha, M. E., *Concepts and Applications of Finite Element Analysis*, 3rd ed., John Wiley & Sons, New York, NY, (1989).

10. Copas, T. L., and Pennock, H. A., "Motor Vehicle Size and Weight Regulations, Enforcement, and Permit Operations," *National Cooperative Highway Research Program Synthesis of Highway Practice*, Report 68, Transportation Research Board, Washington, D.C., (1980).

11. Dodds, R. H., and Lopez, L. A., "A Generalized Software System for Nonlinear Analysis," *International Journal for Advances in Engineering Software*, 2(4), (1980): 161–168.

12. Imbsen and Associates, Inc., "Distribution of Wheel Loads on Highway Bridges," *National Cooperative Highway Research Program*, Project 12–26, Transportation Research Board, Washington, D.C., (1991).

13. Kok, A. W. M., and Vrijman, C. F., "Analysis of continuous structures with the FEM," *ICES STRUDL II*, ICES–Users Group Inc., Cranston, RI, (1985).

14. Loo, Y. C., and Cusens, A. R., *The Finite–Strip Method in Bridge Engineering*, Viewpoint Publications, Oxford, (1978).

15. Marx, et al., "Development of Design Criteria for Simply Supported Skew Slab–and–Girder Bridges," *Final Report*, FHWA/IL/UI–210, (1986).

16. Newmark, N. M., "Design of I–beam Bridges," *Highway Bridge Floor Symposium, Journal of the Structural Division*, American Society of Civil Engineers, Vol. 74, No. 2 (1948): 141–161.

17. *Ontario Highway Bridge Design Code*, Ontario Ministry of Transportation and Communications, Downsview, Onterio, Canada, (1983).

18. Puckett, J. A., *Compound Strip Method for the Analysis of Continuous Elastic Plates*, Str. Research Report No. 48, Civil Engineering Department, Colorado State University, Fort Collins, CO, (1983).

19. Puckett, J. A., and Gutkowski, R. M., "Compound Strip Method for Analysis of Plate Systems," *Journal of the Structural Division*, American Society of Civil Engineers, Vol. 112, No. ST 1 (1986): 121–138.

20. Sanders, W. W., "Distribution of Wheel Loads on Highway Bridges," *National Cooperative Highway Research Program Synthesis of Highway Practice*, Report 111, Transportation Research Board, Washington, D.C., (1984).

21. Sanders, W. W., and Elleby, H. A., "Distribution of Wheel Loads on Highway Bridges," *National Cooperative Highway Research Program*, Report 83, Transportation Research Board, Washington, D.C., (1970).

22. *Standard Specifications for Highway Bridges*, 13th ed., The American Association of State Highway and Transportation Officials, Washington, D.C., (1989).

23. Tarhini, K. M., and Frederick, G. R., "Wheel Load Distribution in I-Girder Highway Bridges," *Journal of the Structural Division*, American Society of Civil Engineers, Vol. 118, No. ST 5 (1992): 1285–1294.

24. Timoshenko, S., and Woinowsky-Krieger, S., *Theory of Plates and Shells*, 2nd ed., McGraw-Hill, New York, NY, (1971).

25. Wiseman, D. L., "Compound Strip Method for the Analysis of Folded Plates," a thesis presented to the University of Wyoming, at Laramie, WY, in partial fulfillment of the requirements for the degree of Master of Science. (1987)

26. Zellin, et al., "Structural Behavior of Beam-Slab Highway Bridges, A Summary of Completed Research and Bibliography," *Fritz Engineering Laboratory Report No. 387.1*, Lehigh University, (1973).

27. Zienkiewicz, O. C., *The Finite Element Method in Engineering Science*, 3rd ed., McGraw-Hill, London, (1977).

SELECTED BIBLIOGRAPHY

American Institute of Steel Construction, *Load and Resistance Factor Design, Manual of Steel Construction*, 1st ed., Chicago: AISC, (1986).

Bakht, B., and Jaeger, L. G., *Bridge Analysis Simplified*, McGraw–Hill, New York, NY, (1985).

Bakht, B., and Moses, F., "Lateral Distribution Factors for Highway Bridges," *Journal of the Structural Division*, American Society of Civil Engineers, Vol. 114, No. ST 8 (1988): 1785–1803.

Beer, F. P., and Johnston, R. E., *Mechanics of Materials*, McGraw–Hill, New York, NY, (1981).

Boresi, A. P., and Sidebottom, O, M., *Advanced Mechanics of Materials*, 4th ed., John Wiley & Sons, New York, NY, (1985).

Boyce, W. E., and Diprima, R. C., *Elementary Differential Equations and Boundary Value Problems*, 4th ed., John Wiley & Sons, New York, NY, (1986).

Cheung, Y. K., *Finite Strip Method in Structural Analysis*, Pergamon Press, Oxford, (1976).

Ghali, A., and Neville, A. M., *Structural Analysis, a Unified Classical and Matrix Approach*, 3rd ed., Chapman and Hall, New York, NY, (1989).

Imbsen and Associates, Inc., "Distribution of Wheel Loads on Highway Bridges," *National Cooperative Highway Research Program*, Project 12–26, Transportation Research Board, Washington, D.C., (1991).

Paz, M., *Structural Dynamics, Theory and Computation*, 3rd ed., Van Nostrand Reinhold, New York, NY, (1991).

Puckett, J. A., Personal Communications, (1992).

Puckett, J. A., and Gutkowski, R. M., "Compound Strip Method for Analysis of Plate Systems," *Journal of the Structural Division*, American Society of Civil Engineers, Vol. 112, No. ST 1 (1986): 121–138.

Timoshenko, S., and Woinowsky–Krieger, S., *Theory of Plates and Shells*, 2nd ed., McGraw–Hill, New York, NY, (1971).

Wiseman, D. L., "Compound Strip Method for the Analysis of Folded Plates," a thesis presented to the University of Wyoming, at Laramie, WY, in partial fulfillment of the requirements for the degree of Master of Science. (1987).